

NSTIF

300010-0

GRANT

10-47-CR

189720

848

ANNUAL REPORT

Measurements of Micrometeorological Parameters for
Testing Large Scale Models

NASA Grant NAG 5-389

Principal Investigator

E. T. Kanemasu

Co-Investigators

Tanvir Demetriades-Shah
David Watts
Dalin Nie
Larry Ballou
Galen Harbers

March 1989

(NASA-CR-184766) MEASUREMENTS OF
MICROMETEOROLOGICAL PARAMETERS FOR TESTING
LARGE SCALE MODELS Annual Report (Kansas
State Univ.) 84 p

CSCL 04B

N89-17384

Unclas

G3/47 0189720

ANNUAL REPORT

Measurements of Micrometeorological Parameters for
Testing Large Scale Models

NASA Grant NAG 5-389

Principal Investigator

E. T. Kanemasu

Co-Investigators

Tanvir Demetriades-Shah

David Watts

Dalin Nie

Larry Ballou

Galen Harbers

March 1989

Subtitle Measurements of Micrometeorological Parameters for Testing Large-scale Models: Estimating Regional Evapotranspiration from Remotely Sensed Data by Surface Energy Balance Models		5. Report Date
Author(s) E. T. Kanemasu		6. Performing Organization Code
Performing Organization Name and Address Evapotranspiration Laboratory Kansas State University Manhattan, KS 66506		8. Performing Organization Report
Sponsoring Agency Name and Address NASA/Goddard Space Flight Center Code 624		10. Work Unit No.
		11. Contract or Grant No. NAG 5-389
		13. Type of Report and Period Covered ANNUAL REPORT
		14. Sponsoring Agency Code NASA/GSFC Code 624

Supplementary Notes
 Technical Monitor
 Dr. Robert Gurney

Abstract

This annual report discusses the work accomplished on the FIFE project.

ORIGINAL PAGE IS
OF POOR QUALITY

Key Words (Suggested by Author(s)) Energy balance, reflectance, surface temperature, grassland	18. Distribution Statement
---	----------------------------

Security Classif. (of this report) Classified	20. Security Classif. (of this page) Unclassified	21. No. of Pages 64	22. Price*
--	--	------------------------	------------

TABLE OF CONTENTS

Introduction.....	4
Chapter 1..... A Comparison of Net Radiation on Slopes	5
Chapter 2..... Site Variability in Soil Heat Flux at FIFE Sites 6 and 30/32	8
Chapter 3..... Comparison of Soil Heat Plate Calibrations	13
Chapter 4..... Modified Heat-Meter Method for Determining Soil Heat Flux	22
Chapter 5..... Soil Water Content Versus Water Potential for FIFE Sites	58
Chapter 6..... 1988 Plant and Soil Data for FIFE Sites	61

Introduction

This document contains the manuscripts and reports during the past year of Grant NAG 5-389. There are six chapters. Three chapters are regarding soil heat flux, and two deal with information about the FIFE sites. The first chapter on net radiation and fourth chapter are being presented at the Agricultural and Forest Meteorology Conference in March, 1989, in Charleston, South Carolina.

Chapter 1

A Comparison of Net Radiation on Slopes

(Presented to Agricultural and Forest Meteorology Conference,
March, 1989, Charleston, SC)

Dalin Nie and E. T. Kanemasu

Kansas State University

1. INTRODUCTION

The importance of radiation balance on slopes has been long recognized. For many years, scientists have attempted to compute the radiation on slopes theoretically (Kondratyev and Manolova, 1960; Liu and Jordan, 1960; Garnier and Ohmura, 1968; Steven and Unsworth, 1980). However, theoretical treatments have not been fully tested with measurements.

In recent years, direct measurements are in greater and greater demand. In order to get the flux on the slope surface, ideally, instruments should be placed parallel to the slope. Because of the difficulty in aligning the radiometer parallel to the slope, it is usually placed horizontal. To get the net radiation for the slope, it is usually assumed that the difference between the horizontal and parallel measurements is only in the direct beam, and one can apply a geometric correction on the beam according to direction of the sun and the slope. However, the assumption has not been adequately tested.

2. MATERIAL AND METHOD

Measurements were made on a 22 degree north-facing slope and a 16 degree south-facing slope in the FIFE site -- the Konza Prairie Natural Research Area, south of Manhattan, Kansas, during 1988. Two double-dome net radiometers (REB Systems) were placed in each slope, one horizontal and one parallel to the slope. In addition, globe and diffuse radiation were also measured horizontally on each slope.

The correction to the slope from horizontal measurement was proceeded as follow:

$$\text{beam (h)} = \text{globe} - \text{diffuse} \quad (1)$$

$$\text{beam (s)} = \text{beam (h)} \times \cos(\theta i) / \sin(\theta se) \quad (2)$$

$$Q(s) = Q(h) - \text{beam (h)} + \text{beam (s)} \quad (3)$$

here, h represents flux as seen on a horizontal surface and s as seen on the slope. θse is the solar elevation, and θi is the angle between the sun's ray and the normal of the slope and $\cos(\theta i)$ is expressed as (Wong, 1979):

$$\cos(\theta i) = \cos(\alpha) \sin(\theta se) + \cos(\theta se) \sin(\alpha) \cos(\theta sa - \beta)$$

α is the angle of the slope, β is the azimuth angle of the slope and θsa is the azimuth angle of the sun.

3. RESULTS AND DISCUSSION

Data measured during daytime of May 12 (88133) and August 14 (88227) were analyzed for the comparison. Fig. 1 presents the diurnal

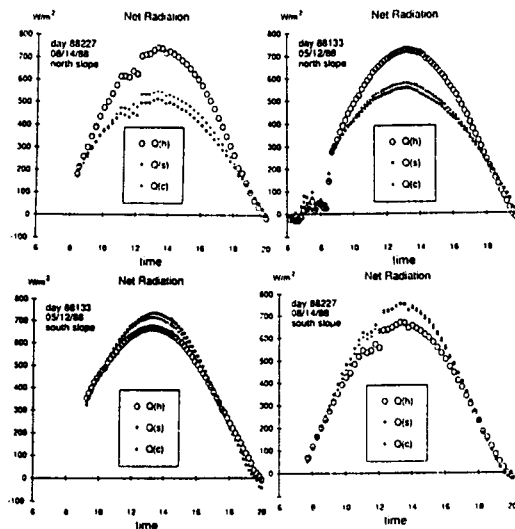


Fig. 1. Comparison of net radiations as horizontal-measured (Q(h)), parallel-measured (Q(s)) and computed (Q(c)) for two slopes.

variations of the net radiation of horizontal-measured (Q(h)), parallel-measured (Q(s)) and computed for the slope using equation (3) (Q(c)) for each slope. The figure shows the computed radiation represents the net radiation on the slope better than the horizontal-measured when compared to the net radiation measured parallel to the slope. The difference between Q(h) and Q(c) can be as large as 200 w/m² in north-facing slope and 80 w/m² in the south-facing slope, depending on time of day and year. The horizontal measurement was greater in midday and smaller early in the morning and late afternoon in the north-facing slope, and the opposite for south-facing slope. This indicates the correction is absolutely necessary if the measurement is made by placing the instrument horizontally.

When the computed Q(c) is compared to the parallel measurement Q(s), the two agreed reasonably well with each other. The south-facing slope showed better agreement, especially on August 14. The computed net radiation (Q(c)) was consistently

ORIGINAL PAGE IS
OF POOR QUALITY

smaller than the parallel-measure $Q(s)$ on the south-facing slope, whereas $Q(c)$ is larger than $Q(s)$ on the north-facing slope. The difference can be over 40 w/m^2 or 8% of $Q(s)$ in the middle day on the north-facing slope. On the south-facing slope, there was also more than 20 w/m^2 of difference (3-4%). Table 1 gives the statistics for linear regression between $Q(c)$ and $Q(s)$. The difference between $Q(c)$ and $Q(s)$ on average for daytime was less than 25 w/m^2 or less than 7%.

Table 1. Statistical comparison of net radiation: $Q(s)$ versus $Q(c)$ (daytime: $Q > 0$)

day	slope	a	b	R^2	error	delta
133	south	0.952***	16***	0.998	-1	-7
227	south	1.003***	-2	0.997	0	-1
133	north	1.082***	-19***	0.998	3	11
227	north	1.093***	-10	0.992	6.3	22

$Q(c) (\text{ w/m}^2) = a * Q(s) (\text{ w/m}^2) + b$
 delta = average $Q(c)$ - average $Q(s)$
 error = (integrated $Q(c)$ - integrated $Q(s)$) / integrated $Q(s)$
 ***, **, * significant at 0.1%, 1%, .5% level, respectively

Comparing the horizontally-measured net radiation between the two slopes, the net radiation on the north-facing slope was greater (Fig. 2a). The difference can be as large as 80 w/m^2 at midday. The total globe radiation was similar for both slopes (Fig. 2b), thus the direct beam radiation was essentially the same for both slopes when measured horizontally. The cause of the difference in net radiation between the two slopes was in long-wave and/or in the reflected short-wave. The difference may account for the difference between the $Q(c)$ and $Q(s)$.

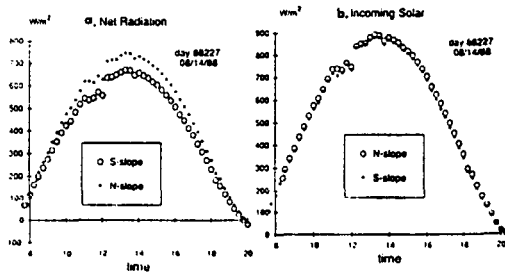


Fig. 2. Radiation comparison between a north-facing slope and a south-facing slope.

4. SUMMARY

1. It is necessary to make corrections for the slope if the net radiation measurements were made horizontally, especially for north-facing slope.
2. The correction in direct beam gives reasonable estimates of net radiation for the slope. However, the correction underestimates the radiation for south-facing slopes and overestimates for north-facing slopes.
3. The correction could be improved if one takes into account the long-wave and reflected short-wave for the slopes.

5. REFERENCES

Garnier, B.J. and Ohmura, A., 1968: A method of calculating the direct shortwave radiation income of slopes. *Journal of Applied Meteorology* 7:769-800.

Kondratyev, K.J. and Manolova, M.P., 1960: The radiation balance of slopes. *Solar Energy* 4:14-19.

Liu, B.Y.H. and Jordan, R.C., 1960: The interrelationship and characteristic distribution of direct, diffuse and total solar radiation. *Solar Energy* 4:1-19.

Steven, M.D. and Unsworth, M.H., 1979: The diffuse solar irradiance of slopes under cloudless skies. *Quarterly Journal of the Royal Meteorological Society* 105:593-602.

Wong, D.M., 1979: Microclimate and microclimate in agricultural field. Agricultural Publisher, Beijing (in Chinese).

Chapter 2

Site Variability in Soil Heat Flux at FIFE Sites 6 and 30/32

**Site Variability in Soil Heat Flux
at FIFE Sites 6 and 30/32**

- a contributing report to the FIFE Surface Flux Group -

by

David Watts
Evapotranspiration Laboratory
Waters Annex
Kansas State University
Manhattan, Kansas 66506
USA
Tel. 913-532-5731

September 23, 1988

At the April 1988 FIFE workshop our group suggested that each PI examine the 'within-site' variability in heat flux at the soil surface using his data acquired during last year. It was further suggested to separate this spatial variability into two components, plate-to-plate variability at plate depth and variability in the layer-averaged soil temperature above plate depth.

Among data collected from FIFE sites 6,8,10,12,14 and 30/32, only data from sites 6 and 30/32 were sufficient to perform a statistical analysis of heat flux at plate depth. None of the site data were sufficient for analysis of the variability in soil temperature.

Site 6 was an upland, ungrazed and unburned site located on the Konza Prairie Natural Area. Data from site 6 were collected by Mr. Dalin Nie of Kansas State University. Site 30/32 was an upland, grazed and burned site located in the southeast quadrant of the overall FIFE area. Data from site 30/32 were collected by Dr. Bill Kustas of the USDA/ARS. Five plates were buried at a depth of 7.5 cm at site 6 and three plates were placed at a 5.0 cm depth at site 30/32. All three of the plates used at site 30/32 were manufactured by Micromet Systems, Inc. Two of the five plates in use at site 6 were also from Micromet; the rest were supplied by Dr. Marcel Fuchs. By employing different types of plates calibrated in different systems in order to measure heat flux at the same site, the question is raised as to whether the two types would measure the same flux in exactly the same location. For a discussion of this topic please refer to the Surface Flux Group report entitled, "Comparison of Soil Heat Flux Plate Calibrations" (to be distributed at the November 1988 FIFE workshop). In this analysis no difference is assumed. It is also assumed that the distance between plates within a site was large enough so that measurements from each plate could be considered statistically independent of the

others at any given time. Golden Day No. 2, day 192, was selected for the analysis.

At first, the standard analysis-of-variance model was considered but then rejected as a method of detecting significant differences in soil heat flux because of the temporal autocorrelation in the 24-hour data set. Instead, half-hourly data from both sites were selected from four, one-hour periods during day 192 from which hourly means and standard deviations in heat flux were calculated. Results are shown in the table that follows. The tabular data clearly indicate much greater within-site variability in soil heat flux at site 30/32, which was recently grazed and burned, compared to the variability at site 6 which had not been grazed or burned in at least ten years. This is especially evident during the midday period. However, the effect of burning or grazing may be confounded somewhat by the fact that the plates at site 6 were buried more deeply than at site 30/32. There is also the complication that each of the five plates at site 6 was purposely located where the amount of vegetative canopy cover was judged as the average for the site.

Golden Day 2 (day 192)

<u>site number</u>	<u>hour (CDT)</u>	<u>mean flux (Wm^{-2})</u>	<u>std. dev. (Wm^{-2})</u>
6	0100 - 0200	4.4	0.9
	0700 - 0800	7.9	1.4
	1300 - 1400	-26.1	3.1
	1900 - 2000	-11.4	5.3
30/32	0100 - 0200	21.7	5.0
	0700 - 0800	14.7	4.6
	1300 - 1400	-101.8	39.2
	1900 - 2000	-10.3	9.0

Chapter 3

Comparison of Soil Heat Plate Calibrations

Comparison of Soil Heat Flux Plate Calibrations

- a report to the FIFE Surface Flux Group -

by

David Watts
Evapotranspiration Laboratory
Waters Annex
Kansas State University
Manhattan, Kansas 66506
USA
Tel. 913-532-5731

September 12, 1988

At the April 1988 FIFE workshop our group decided that a comparison of soil heat flux plate calibrations was necessary so that we could try to evaluate the level of accuracy and precision in our soil heat flux measurements. Many of the plates used in 1987 were manufactured by Micromet Systems, Inc. and calibrated in a water-saturated, glass bead medium by Dr. Leo Fritschen. Other plates of different construction used by the KSU team were made and calibrated by Dr. Marcel Fuchs in a dry, quartz sand. And others of various shapes and thermal conductivities were probably in use by other investigators as well. The question we wish to address in this report is how well do these plate calibrations compare.

To make a truly accurate comparison is not practical in our case. Assuming the standard, steady-state method of calibration we would have to examine how each plate is calibrated in each device. Is the plate aligned perpendicular to the direction of heat flow? Is the power supply constant over time? Is the calibration device sufficiently insulated to minimize edge heat loss? Is the system allowed to reach steady-state so that a highly uniform heat flux can develop? The list of questions is virtually endless, but nevertheless we need to start somewhere.

One major source of discrepancy between calibrations can occur when a plate is placed in two media of differing thermal conductivities. Philip's theory of heat flux meters should resolve such a source (Philip, 1961). His theory forms the basis for the analysis in this report. Briefly he states that the ratio, F , of mean flux density through the plate to the flux density through the medium at a large distance from the plate is related to the ratio, E , of plate conductivity to medium conductivity by the equation

$$F = \frac{E}{1 + (E-1)H} \quad (1)$$

where H is solely dependent upon plate geometry. For square plates H can be approximated by the expression

$$H = 1.70 \frac{T}{L} \quad (2)$$

where T is the plate thickness and L is its side length. This theory is saying in effect that if we know the dimensions and thermal conductivity of the plate as well as the conductivity of the surrounding medium, then we can predict the relative perturbation of the medium's heat flux field inside the plate. Since the heat flux perturbation varies with medium conductivity, if we insert a plate in medium one, then

$$F_1 = \frac{G_{p1}}{G_1} = \frac{C_p V_1}{C_1 V_1} = \frac{C_p}{C_1} \quad (3)$$

If we insert it into medium two, then

$$F_2 = \frac{G_{p2}}{G_2} = \frac{C_p}{C_2} \quad (4)$$

where C is a calibration coefficient in, say, $Wm^{-2}mV^{-1}$, V is the millivolt signal of the plate and the subscript p denotes within the plate. Dividing eq. 3 by eq. 4 yields

$$\frac{F_1}{F_2} = \frac{C_2}{C_1} \quad (5)$$

Equation 5 provides us with a means of comparing the ratio of measured calibration coefficients of a plate placed in two different media with the ratio

predicted by Philip's theory.

Four heat flux plates (two of them from Micromet Systems, one from Dr. Fuchs and one fabricated in our lab) were circulated among as many as eight different calibration systems. In order to compare measured versus predicted calibration ratios for more than two systems a reference system was required. Dr. Fuchs' calibration device containing a dry, quartz sand medium was chosen. Table 1 lists the values of relevant parameters for each plate or meter. The thermal conductivities of the two Micromet plates are based on the conductivity values of the epoxy supplied by the manufacturer. Dr. Fuchs' plate conductivity is that of the glass component of his plate. The conductivity of the plate from the ET Lab was determined using an electrical resistance analog approach. Calibrations with all systems employed the steady-state method as far as we know. Medium thermal conductivities are provided in Table 1. Associated with each value is a letter code designating the system used. The code is as follows:

- a - dry, quartz sand in Fuchs' device
- b - grinding carbide in Fuchs' device
- c - water-saturated, glass beads in Fritschen's device
- d - dry, quartz sand in ET Lab's device
- e - dry, quartz sand in a 2nd ET Lab device designed by Dave Watts
- f - water-saturated, glass beads in above device
- g - water-saturated, quartz sand in above device
- h - dry sand in Dr. Bob Reginato's device.

Table 1 also gives computed values of E and of F using equation 1.

- 4 -

Table 2 lists the calibrations and when they were conducted. Measured calibration coefficient ratios were then determined by dividing a given plate calibration in one medium by the reference calibration in (a). Calibration ratios according to Philip's theory were derived in a similar fashion from the values listed in Table 1. If Philip's theory is correct and no other sources of error exist in our calibrations, then the measured calibration ratios should equal those derived using Philip's theory. In some cases they do, while in others they do not as shown in Figure 1. Note that calibration ratios from systems (a) and (d) agree quite well using all four plates. This is an encouraging sign because these two systems are similar in construction and contain the same type of medium.

These results suggest that there are definitely other sources of discrepancy in our calibrations besides the perturbation of the heat flow by the plate. It appears that these sources when lumped together are at least equal in magnitude to the perturbation source. We think that one of the largest sources is the edge heat loss through the calibration device or box. We suggest subtracting an estimate of the heat loss rate from the total applied power before computing a calibration. Alternatively, the thermal conductivity of the medium could be determined using the transient, line source or probe method from which the heat flux density could be evaluated from the temperature gradient across the medium.

Philip, J.R. 1961. The theory of heat flux meters. *J. Geophys. Res.* 66:571-579.

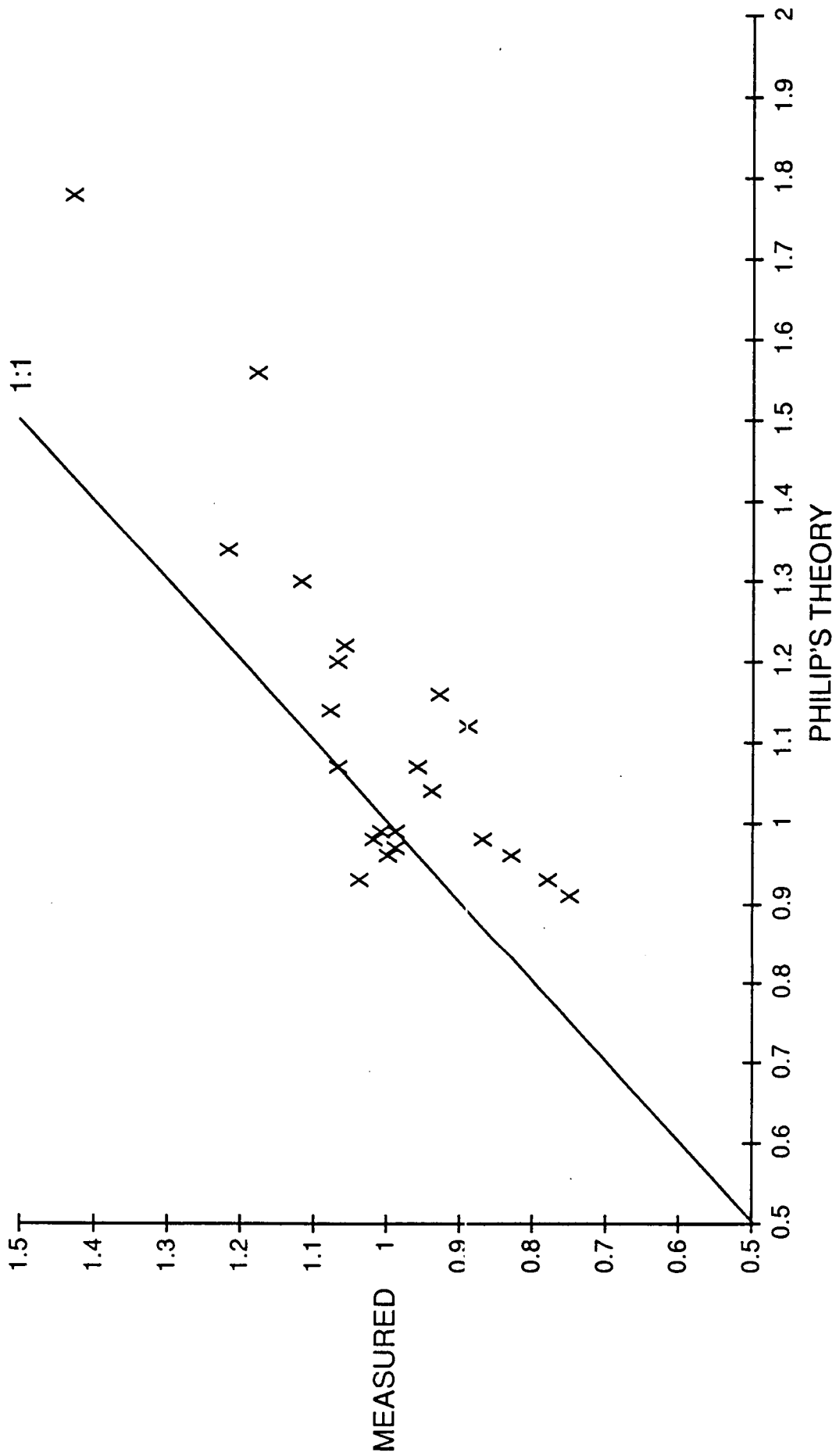
TABLE 1

ID No. and Source	Meter Shape	Meter Dimensions (mm)	Meter Shape Factor H	Meter Thermal Conductivity [$\text{Wm}^{-1}\text{C}^{-1}$]	Medium Thermal Conductivity [$\text{Wm}^{-1}\text{C}^{-1}$]	E	F
85017 L.Fritschen	square	32x32x5.1	0.730	0.48	0.42 (a)	1.14	1.03
					0.31 (b)	1.55	1.11
					0.94 (c)	0.51	0.79
					0.37 (d)	1.30	1.07
					0.27 (e)	1.78	1.13
					0.71 (f)	0.68	0.89
					1.77 (g)	0.27	0.58
87054 L.Fritschen	square	33x33x5.1	0.737	0.69	0.42 (a)	1.64	1.11
					0.94 (c)	0.73	0.91
					0.37 (d)	1.86	1.14
					0.27 (e)	2.56	1.19
					0.71 (f)	0.97	0.99
					1.77 (g)	0.39	0.71
					64 M. Fuchs	rectangular	30x80x2.8
0.94 (c)	0.74	0.97					
0.37 (d)	1.89	1.05					
0.29 (h)	2.41	1.06					
0.27 (e)	2.59	1.06					
0.71 (f)	0.99	1.00					
1.77 (g)	0.40	0.87					
16 ET Lab	square	34x36x6.8	0.670	1.7	0.42 (a)	4.05	1.33
					0.94 (c)	1.81	1.17
					0.37 (d)	4.59	1.35
					0.27 (e)	6.30	1.38
					0.71 (f)	2.39	1.24
					1.77 (g)	0.96	0.99

TABLE 2

ID No. and Source	Medium Thermal Conductivity [Wm ⁻¹ C ⁻¹]	Calibration [Wm ⁻¹ mv ⁻¹]	(Date)	Calibration Ratio:	
				Measured	Philip's Theory
85017 Fritschen	0.42 (a)	29.5	(7/87)	--	--
	0.31 (b)	30.7	(7/87)	1.04	0.93
	0.94 (c)	33.0	(2/88)	1.12	1.30
	0.37 (d)	29.5	(1/88)	1.00	0.96
	0.27 (e)	22.1	(7/88)	0.75	0.91
	0.71 (f)	27.3	(7/88)	0.93	1.16
	1.77 (g)	42.3	(7/88)	1.43	1.78
87054 Fritschen	0.42 (a)	39.3	(7/87)	--	--
	0.94 (c)	41.6	(2/88)	1.06	1.22
	0.37 (d)	39.0	(1/88)	0.99	0.97
	0.27 (e)	30.8	(7/88)	0.78	0.93
	0.71 (f)	34.9	(7/88)	0.89	1.12
	1.77 (g)	46.3	(7/88)	1.18	1.56
	64 Fuchs	0.42 (a)	129.0	(?)	--
0.94 (c)		138.0	(2/88)	1.07	1.07
0.37 (d)		130.0	(1/88)	1.01	0.99
0.29 (h)		131.0	(5/87)	1.02	0.98
0.27 (e)		112.0	(7/88)	0.87	0.98
0.71 (f)		121.0	(7/88)	0.94	1.04
1.77 (g)		139.0	(7/88)	1.07	1.20
16 ET Lab	0.42 (a)	24.0	(7/87)	--	--
	0.94 (c)	25.9	(2/88)	1.08	1.14
	0.37 (d)	23.8	(1/88)	0.99	0.99
	0.27 (e)	19.9	(7/88)	0.83	0.96
	0.71 (f)	23.1	(7/88)	0.96	1.07
	1.77 (g)	29.4	(7/88)	1.22	1.34

FIGURE 1



Chapter 4

Modified Heat-Meter Method for Determining Soil Heat Flux

1 **Title: Modified Heat-Meter Method for Determining Soil Heat Flux***

2
3
4
5
6 **Authors: D.B. Watts**, E.T. Kanemasu and C.B. Tanner**

7 **Evapotranspiration Laboratory**

8 **Waters Annex**

9 **Kansas State University**

10 **Manhattan, Kansas, U.S.A. 66506**

11
12
13
14
15 **Date: January 23, 1989**

16
17 **Submitted to: Agricultural and Forest Meteorology Journal**

18 **Elsevier Science Publishers B.V., Amsterdam, Netherlands**

19
20
21
22 _____
23 *** Contribution No. ____ of the Kansas Agricultural Experiment Station.**

24 **** corresponding author**

1
2
3
4
5
6
7
8
9
10
11
12
13
14
15
16
17
18
19
20
21
22
23
24
25
26
27

Abstract:

The theory of heat-flux meters describing the perturbation of a uniform, steady heat flux through a porous medium (soil) by a meter of different thermal conductivity is tested and confirmed under laboratory conditions. From the theory an equation is derived for determining the heat flux density through the medium which is more accurate than direct calibration equations. The medium heat flux density is found by first calibrating a heat-meter independently in two other media differing in thermal conductivity. Then once the meter is inserted into the medium of interest, its signal and the temperature gradient in the direction of heat flow at a large distance from the meter are measured. The method should serve to provide for more accurate assessment of the energy budget of the earth's surface.

1 I. Introduction

2 Accurate measurement of heat flow through soils is important in assessing
3 the energy budget of bare or thinly-vegetated soil surfaces. Computed as the
4 residual term of the hourly energy budget the evapotranspiration rate from such
5 surfaces depends critically upon surface soil heat flux. Because of the coupling
6 between heat and moisture movement in unsaturated soils, heat flux measure-
7 ment is also useful in modeling the flux of soil moisture.

8 One commonly used method of determining soil heat flow is the flux-plate
9 or heat-meter method. A heat-flux meter, a flat piece of solid material with rigid
10 shape and constant thermal conductivity, is inserted in the soil with its large
11 dimensional area in the plane perpendicular to the direction of heat flow. The
12 flow of soil heat produces a temperature gradient across this plane or the shortest
13 dimension of the meter. A sensing element embedded within the meter (usually
14 a thermopile) detects the temperature difference across the meter generating a
15 signal (Fuchs,1986).

16 Heat-flux meters are usually calibrated either in a dry sand, soil or some
17 other soil-like porous medium in the laboratory under controlled, steady-state
18 thermal conditions. The medium contained by a rectangular or square box is
19 heated on one side and/or cooled on the other developing a uniform, steady,
20 known heat flux density throughout the medium. The calibration coefficient of
21 the heat flux meter is found by dividing the known flux density by the meter sig-
22 nal. Uniformity in the flux density within the medium requires two conditions.
23 One is that insulation of the edges of the box should be sufficient to prevent any
24 lateral heat loss. The other places a maximum limit on the number of meters
25 with thermal conductivity differing from that of the medium which can be cali-
26 brated simultaneously in the box. Several designs of calibration boxes have
27 been reported (Fuchs and Tanner,1968;Fuchs and Hadas,1973;Biscoe et

1 al.,1977).

2 The meter method is the most convenient method to use in the field since it
3 provides a direct reading of heat flux density. When the intended purpose is to
4 monitor the soil surface energy budget, it is generally best to install meters at a
5 depth of 5 to 10 cm leaving the evaluation of the flux divergence (or heat
6 storage) between the meter and surface to calorimetry in situ (Fuchs and
7 Tanner,1968). Because of its simplicity and the fact that few auxiliary measure-
8 ments are required, the method is well suited for long-term assessment of soil
9 heat flux density (Fuchs,1986).

10 Heat flux density readings are best obtained when the meters are carefully
11 constructed, calibrated and installed in the soil (Kimball and Jackson,1979).
12 This is especially true of the installation procedure. Incomplete contact between
13 the soil matrix and meter surfaces or poor alignment of the meter with the direc-
14 tion of soil heat flow always reduces the response of the heat flux transducer
15 (Philip,1961;Fuchs and Hadas,1973).

16 Unfortunately, as with all methods of obtaining soil heat flux density this
17 method monitors only the sensible heat component of the energy flux through
18 soils. The latent heat or the water vapor flux component may be comparable
19 near the surface of a warm, drying soil where the water potential gradient is
20 greatest in magnitude. In addition, water vapor from the soil may condense on
21 the meter causing an erroneous reading (Fuchs,1986).

22 When the thermal conductivity of the soil is lower (or higher) than that of
23 the meter, heat flux converges toward (or diverges around) one side of the meter
24 and diverges away from (or converges around) the opposite side. Philip (1961)
25 developed a theoretical model of how soil heat flow is perturbed by a heat flux
26 meter in which he related the ratio F of mean flux density through the meter

27 over the flux density through the medium to the ratio E of meter thermal

1 conductivity over medium thermal conductivity and a geometry factor H .

$$2 \quad F = \frac{E}{1 + (E-1)H} \quad (1)$$

3
4 Strictly speaking, the equation is exact only for a meter that is an ellipsoid in
5 shape so that for flat meters it is only an approximation. For thin square meters
6 Philip (1961) approximated H as

$$7 \quad H \approx 1 - 1.70 \frac{T}{L} \quad (2)$$

8 where T is the meter thickness and L is its side length. For disc-shaped meters
9 he approximated

$$10 \quad H \approx 1 - 1.92 \frac{T}{D} \quad (3)$$

11 where D is the diameter of the meter.

12
13 Mogensen (1970) tested Philip's equation, rewritten as

$$14 \quad F^{-1} = H + (1-H)E^{-1} \quad (4)$$

15
16 He inserted a meter in media of widely different thermal conductivities and
17 found that the relationship between F^{-1} and E^{-1} was linear as predicted by eq.
18 4; however, his experimental value of F^{-1} underestimated the theoretical value
19 by about 12 percent. He attributed this error to the heterogeneous structure of
20 the meter.

21 Philip (1961) recommended that meters should be constructed to be as thin
22 as possible (H close to unity) with the greatest possible thermal conductivity (E
23 large) in order to minimize the perturbation of soil heat flux (to make F close to
24 unity) thus improving measurement accuracy. But current technology limits how
25 thin meters of high thermal conductivity can be made that still produce a meas-
26 ureable signal.

1 In this paper we propose a solution to this problem. By writing Philip's
 2 equation for a meter inserted into two media of differing thermal conductivities
 3 we derive an equation for the heat flux density in a third medium of intermediate
 4 conductivity. The equation is tested under laboratory conditions and is shown to
 5 yield a more accurate estimate of medium heat flux than the flux-plate or heat-
 6 meter method where no information about the medium is used. The experiment
 7 demonstrates that meters do not have to be made extremely thin or thermally
 8 conductive to produce accurate measurements of medium heat flux.

9 II. Derivation of Medium Heat Flux Density

10 Equation 1 is exact for any ellipsoid object or meter with homogeneous,
 11 isotropic thermal conductivity oriented with a principal axis parallel to the direc-
 12 tion of heat flow at large distances from the meter. The surrounding medium is
 13 also assumed to be a homogeneous, isotropic thermal conductor of infinite
 14 volume.

15 If an ellipsoid meter of conductivity, K_p , is inserted in one such medium of
 16 conductivity, K_1 , subjected to a steady, uniform heat flux density, G_1 , then the
 17 inverse of eq. 1 is

$$18 \quad \frac{G_1}{G_{p1}} = \left[1 + \left(\frac{K_p}{K_1} - 1 \right) H \right] \cdot \frac{K_1}{K_p} \quad (5)$$

19 where G_{p1} is the heat flux density through the meter and the subscript p
 20 denotes within the meter. The typically measured calibration coefficient, C_1
 21 ($\text{Wm}^{-2}\text{V}^{-1}$), is found from the equation

$$22 \quad G_1 = C_1 \cdot V_1 \quad (6)$$

23 where V_1 is the voltage signal in medium one. At the same time, G_{p1} defines
 24 the meter sensitivity, C_p , by the equation

$$25 \quad G_{p1} = C_p \cdot V_1 \quad (7)$$

1 Then

$$2 \quad \frac{G_1}{G_{p1}} = \frac{C_1}{C_p} \quad (8)$$

3
4 Substituting eq. 8 into eq. 5 yields

$$5 \quad \frac{C_1}{C_p} = \left[1 + \left[\frac{K_p}{K_1} - 1 \right] H \right] \cdot \frac{K_1}{K_p} \quad (9)$$

6
7 Similarly, if the same meter is placed in a second medium of thermal con-
8 ductivity, K_2 , and flux density, G_2 , its calibration coefficient, C_2 , is defined by

$$9 \quad G_2 = C_2 \cdot V_2 \quad (10)$$

10 where V_2 is the voltage signal in medium two. Simultaneously, the heat flux
11 density through the meter in medium two is:

$$12 \quad G_{p2} = C_p \cdot V_2 \quad (11)$$

13 Thus

$$14 \quad \frac{G_2}{G_{p2}} = \frac{C_2}{C_p} \quad (12)$$

15 So by analogy with eq. 5 and substituting from eq. 12

$$16 \quad \frac{C_2}{C_p} = \left[1 + \left[\frac{K_p}{K_2} - 1 \right] H \right] \cdot \frac{K_2}{K_p} \quad (13)$$

17 Dividing eq. 9 by eq. 13 gives

$$18 \quad \frac{C_1}{C_2} = \frac{1 + \left[\frac{K_p}{K_1} - 1 \right] H}{1 + \left[\frac{K_p}{K_2} - 1 \right] H} \cdot \frac{K_1}{K_2} \quad (14)$$

19 This equation can be solved for K_p , the thermal conductivity of the meter,

$$20 \quad K_p = \frac{1-H}{H} \cdot \left[\frac{K_1 C_2 - K_2 C_1}{C_1 - C_2} \right] \quad (15)$$

1 Now suppose that the meter is inserted into a third medium of conductivity,
 2 K_0 , with flux density, G_0 , defining the calibration coefficient, C_0 , via the equa-
 3 tion

$$4 \quad G_0 = C_0 \cdot V_0 \quad (16)$$

5 where V_0 is the voltage signal in medium three. By analogy with eq. 14

$$6 \quad \frac{C_1}{C_0} = \frac{1 + \left[\frac{K_p}{K_1} - 1 \right] H}{1 + \left[\frac{K_p}{K_0} - 1 \right] H} \cdot \frac{K_1}{K_0} \quad (17)$$

10 Also we may write from eq. 16

$$11 \quad C_0 = - \frac{K_0}{V_0} \cdot \frac{\Delta T}{\Delta z} \Big|_{\infty} \quad (18)$$

13 where $\Delta T/\Delta z \Big|_{\infty}$ is the temperature gradient in medium three in the direction of
 14 heat flow at large distances from the meter. Using eqs. 15, 17 and 18 we can
 15 solve for the thermal conductivity and heat flux density of the third medium
 16 independently of K_p or H .

$$17 \quad K_0 = \frac{C_1 K_2 - C_2 K_1}{C_1 - C_2 + \frac{K_1 - K_2}{V_0} \cdot \frac{\Delta T}{\Delta z} \Big|_{\infty}} \quad (19)$$

20 and

$$21 \quad G_0 = \frac{C_2 K_1 - C_1 K_2}{\frac{C_1 - C_2}{(\Delta T/\Delta z) \Big|_{\infty}} + \frac{K_1 - K_2}{V_0}} \quad (20)$$

24 III. Design of the Calibration Box

25 Philip's theory of heat-flux meters necessitates the following two criteria for
 26 the appropriate design of the calibration box:
 27

1 (1) a steady, uniform heat flux through the depth of the purely conductive cali-
2 bration medium; and

3 (2) the region of heat flux perturbation surrounding the meter is completely con-
4 tained by the medium and is unaffected by the presence of other meters or
5 nearby walls with thermal conductivities different from that of the medium.

6 In order to meet the first criterion a square heat flow box (55 by 55 by 27
7 cm O.D.) was built. Its interior bottom and sides were lined with a 10 cm thick-
8 ness of rigid Blueboard insulation (Dow Chemical Co.) which has a thermal con-
9 ductivity of about $0.028 \text{ Wm}^{-1}\text{C}^{-1}$. A square electrical heater plate (30.6 by
10 30.6 by 0.3 cm) rested flat on top of the bottom portion of the insulation. The
11 heater plate design is similar to that described by Fuchs and Tanner (1968). We
12 placed a sealed, water-tight box with acrylic walls and aluminum base (30.6 by
13 30.6 by 8 cm) flush on top of the heater plate. Both walls and base were 0.3 cm
14 thick. The box was filled with calibration medium and covered with a flat,
15 heavy-gauge aluminum lid.

16 The large thermal resistance of the side insulation directed most of the heat
17 flux from the heater upward through the medium minimizing lateral heat flux
18 and helping to preserve uniformity of heat flux density through the depth of the
19 medium. This was substantiated by measurements of the temperature difference
20 between the lid center and edge which was only 3 to 5 percent of the tempera-
21 ture difference across the depth of the medium. (See Fig. 1.) A regulated
22 Hewlett-Packard Harrison 6284A DC power supply to the heater plate produced
23 steady power which varied less than 0.1 percent during each calibration run.
24 Power to the heater was computed from the voltage measured across the heater
25 leads and from the heater element's electrical resistance measured with a Wheat-
26 stone bridge. The heat flux from the box exterior was dissipated to the sur-
27 rounding room with fan-circulated air set to $20 \text{ C} \pm 1.0 \text{ C}$.

1 From temperature measurements using five copper-constantan thermocou-
2 ples (0.013 cm dia. wire) placed at points along the inner and outer surfaces of
3 the insulation (shown in Fig. 1) and the geometry of the box, nodal values of the
4 temperature gradient normal to the exterior surfaces of the insulation were calcu-
5 lated using a numeric, steady-state, finite-element model. These gradient values
6 were integrated over each surface and multiplied by the approximate thermal
7 conductivity of the insulation. Heat loss rates from each surface including the
8 top of the acrylic walls were then summed over all surfaces to obtain an esti-
9 mate of the total heat loss rate (Table 1).

10 The net heat flux through the media was calculated as the difference
11 between the total applied power and the total loss rate. Dividing the net flux by
12 the horizontal cross-sectional area of the medium (0.0939 m^2) provided the
13 mean heat flux density, G . Division by the voltage signal of an inserted meter
14 gave the meter calibration. We noted that simultaneous insertion of up to four
15 meters had no discernible effect on the temperature profile across both the
16 medium and insulation. Meter sizes are listed in Table 3 and meter spacing is
17 reported later in this section. The thermal conductivity of a medium, K , was
18 found as $-G/(\Delta T/\Delta z)$ where Δz is the depth of the medium and ΔT is the mean
19 temperature difference across it as measured by four thermocouples shown in
20 Fig. 1. Listed in Table 1 are the three media used in the experiment including
21 some of their physical characteristics and thermal conductivities. Power applied
22 to the heater plate was adjusted for each medium so that all meters were main-
23 tained at the same temperature of $37.5 \text{ C} \pm 1.0 \text{ C}$ during all calibration runs.
24 Radiative transfer was negligible and Grashof numbers for both air- and water-
25 filled media were four to five orders of magnitude below the convection thresh-
26 hold.

1 The depth of the calibration media in the box and spacing of the meters
 2 from each other or from walls must allow the heat flow pattern to develop
 3 around the meter as if it were alone in a medium of infinite volume. We use the
 4 complete solution of Laplace's equation for the temperature field both inside and
 5 outside an oblate spheroid (Fig. 2) given by Carslaw and Jaeger (1959, pp.425-
 6 429). We are interested in the case where the c axis (Fig. 2) is aligned parallel
 7 to the direction of heat flow (z-direction) at large distances from the spheroid.
 8 This in effect simulates the system of a flat heat-flux meter oriented perpendicu-
 9 lar to the large-scale direction of heat flow. Philip (1961) used the temperature
 10 solution for inside the oblate spheroid to derive eq. 1 where

$$11 \quad H = \frac{1}{1-(c/a)^2} - \frac{c/a}{[1-(c/a)^2]^{3/2}} \cdot \tan^{-1} \left[\left[\frac{1}{(c/a)^2} - 1 \right]^{1/2} \right] \quad (21)$$

12
 13 In a similar fashion we can use the complete temperature solution outside
 14 the spheroid to derive the temperature gradient in the z-direction for the locus of
 15 points along the x- and z-axes. The pair of equations for the temperature gra-
 16 dient are:

$$17 \quad \frac{\partial T}{\partial z} \Big|_{x=0} = \frac{\partial T}{\partial z} \Big|_{\infty} \cdot (1 + P(0,z)) \quad \text{for } |z| \geq c \quad (22)$$

18 and

$$19 \quad \frac{\partial T}{\partial z} \Big|_{z=0} = \frac{\partial T}{\partial z} \Big|_{\infty} \cdot (1 + P(x,0)) \quad \text{for } |x| \geq a \quad (23)$$

20 where the perturbation factor, $P(x,z)$, is defined as

$$21 \quad P(0,z) = \frac{E-1}{1 + (E-1)H} \cdot$$

$$22 \quad \left\{ \frac{a^2 c}{(a^2 - c^2)^{3/2}} \cdot \tan^{-1} \left[\left[\frac{a^2 - c^2}{z^2} \right]^{1/2} \right] - \left[\frac{a^2 c}{a^2 - c^2} \right] \left[\frac{z}{a^2 - c^2 + z^2} \right] \right\} \quad (24)$$

1 and

$$2 \quad P(x,0) = \frac{E-1}{1 + (E-1)H} .$$

$$3 \quad \left\{ \frac{a^2c}{(a^2-c^2)^{3/2}} \cdot \tan^{-1} \left[\left[\frac{a^2-c^2}{c^2-a^2+x^2} \right]^{1/2} \right] - \left[\frac{a^2c}{a^2-c^2} \right] \left[c^2-a^2+x^2 \right]^{-1/2} \right\} (25)$$

4 , respectively.

5
6 With $P(x,z)$ quantified we need to set a tolerance level for P which
7 defines a distance from the center of the meter in both the x- and z-directions
8 beyond which the perturbation is negligible. Based on the experimental errors
9 likely in other phases of the experiment this level was set at ± 3 percent.

10
11 In order to apply the theory we had to find the correct shape and size of an
12 oblate spheroid that generates the same perturbation at the same distance from
13 its center as a typical circular or square meter. Philip (1961) provided approxi-
14 mations for a suitable shape of the spheroid in terms of the geometric factor, H .
15 (See Philips' approximations (2) and (3).) Numeric modeling of the ratio F for
16 circular-disc meters over the typical range of soil-meter values of E and
17 thickness-to-diameter ratio confirmed that Philip's approximation of H was valid
18 for thin meters but underestimated F by 15 percent for thick meters at $E < 1$.
19 Better overall approximations accurate to within ± 5 percent according to the
20 numeric model are that for disc-shaped meters

$$21 \quad \frac{c}{a} \approx 1.50 \cdot \frac{T}{D} \quad (26)$$

22 and likewise for thin square meters

$$23 \quad \frac{c}{a} \approx 1.33 \cdot \frac{T}{L} \quad (27)$$

24 where either of these approximations may be substituted into eq. 21 to obtain a
25 more accurate H factor.

1 Next, we assumed that the volume of the best-shaped spheroid is equal to
2 the volume of the meter so that for the disc-shaped meter:

$$3 \quad c = \left[\frac{3}{16} \cdot D^2 T \cdot \left(\frac{c}{a} \right)^2 \right]^{1/3} \quad (28)$$

4
5 For the square meter D^2 is replaced by $4L^2/\pi$ in eq. 28. Substituting eq. 26 into
6 both eq. 28 and the exact expression for H (eq. 21) we can solve for $P(x,z)$
7 using eqs. 24 and 25. Additional numeric modeling of the heat flux perturbation
8 in the medium surrounding disc-shaped meters confirmed the analytic solution of
9 $P(x,z)$ at intermediate distances from the center of the meter. The results for
10 thin square meters should be similar.

11 We wished to find among other dimensions the minimum depth of medium
12 required to completely envelop the region of perturbed heat flow by examining
13 cases when this perturbation is greatest in magnitude. The distance outward
14 from the origin (center of meter) along the x and z-axes to the points where the
15 P value is ± 0.03 were then determined for the largest meters used in the experi-
16 ment that had a high ratio of thickness to length for two, opposite extreme cases:
17 (i) the meter of lowest conductivity inserted in the medium with the highest con-
18 ductivity;
19 (ii) the meter of highest conductivity inserted in the medium with the lowest
20 conductivity.

21 Results are shown in Table 2 for square meters in both cases. The pertur-
22 bation limits required that all meters must be buried midway between the top
23 and bottom of the medium and that the medium be at least 66 mm in depth. We
24 chose a depth of 75 mm for our media. The limits further demanded that no
25 meter be any closer than 33 mm from any side wall and that all meters be
26 spaced at least 66 mm apart on centers. We placed all meters at least 50 mm
27

1 from the nearest wall and at least 80 mm apart on centers (or about 50 mm from
2 edge to edge).

3 **IV. Calibration Procedure**

4 A total of seven meters of different shape, size and thermal conductivity
5 were selected for the experiment as shown in Table 3. The H factor for F.#64
6 is not given because its shape does not resemble that of an oblate spheroid.
7 Meter thermal conductivities are estimates supplied by the manufacturers. The
8 meter fabricated at the Evapotranspiration Laboratory at Kansas State University
9 (ETL) was composed of a highly sensitive Peltier cooler transducer
10 (MELCOR, Inc., Trenton, NJ, USA; Model No. CP1.4-71-06L). Weaver and
11 Campbell (1985) discuss its merits as a soil heat flux sensor including its rela-
12 tively low cost. We impregnated and encapsulated this transducer in a very
13 highly conductive epoxy (Stycast 2850FT with catalyst No.
14 11, Emerson & Cuming, Inc., Northbrook, IL, USA).

15 The calibration box was filled with one of three media to a depth of about
16 75 mm. With each additional 25 mm layer added, the medium was tamped in
17 order to remove any large air gaps. The set of meters described above were
18 divided into two groups, as indicated in Table 3, and each group was run as a
19 separate calibration. Meters were spaced adequately from each other as well as
20 from the walls and aligned parallel to the heater plate at mid-depth. The top
21 surface of the medium was smoothed and covered with the aluminum lid. Meter
22 leads exited the medium at the corners of the lid and any heat flow outward
23 along them was assumed negligible. Following each calibration run all meters
24 were inspected for proper location and orientation in the medium.

25 Two of the three media used were saturated with distilled water. Water
26 was added slowly via plastic tubing to the bottom of the medium allowing it to
27 gradually approach saturation. The water supply was stopped once the water

1 level reached the top surface of the medium. To prevent evaporative losses all
2 edges of the lid were sealed to the acrylic side walls with tape. Several small
3 holes drilled through the lid to view the water level were also sealed. During
4 each calibration run about five milliliters of water were added to the medium
5 daily to maintain saturation.

6 Steady electrical power was applied to the heater plate for at least 48 hours
7 before steady-state thermal conditions were achieved in the medium and calibra-
8 tion box prior to each run. Then individual meter voltage signals and system
9 temperatures were collected by a Hewlett-Packard HP3421A data acquisition
10 unit and stored in modular RAM on a Hewlett-Packard HP71B microcomputer.
11 Data were recorded once every hour for a period of 24 hours. A total of six
12 calibration runs were conducted during the experiment.

13 V. Results

14 Results of the pair of calibration runs in each medium are given in Table 4
15 including G , the temperature difference, ΔT (mean of lid center and edge tem-
16 peratures minus the mean of base plate center and edge temperatures), across the
17 depth of the medium, Δz , and the resulting vertical temperature gradient,
18 $\Delta T / \Delta z |_{\infty}$.

19 In Table 5 we list for each meter its calibration in dry sand, C_1 , and in
20 saturated sand, C_2 . Also shown for the saturated glass beads medium are the
21 corresponding meter signal, V_0 , and heat flux density, G_0 , predicted from eq.
22 20.

23 Table 6 shows predicted values of heat flux density from the output of each
24 meter embedded in the saturated glass beads medium using three different tech-
25 niques: (1) using the meter calibration in dry sand; (2) using the calibration in
26 saturated sand; and (3) using eq. 20. The percentage deviation from the meas-
27

1 ured heat flux density of 133 Wm^{-2} (Table 4) is given in parentheses next to
2 each calculated G . Eq. 20 is a better predictor of heat flux density in saturated
3 glass beads than direct calibrations. The overall mean flux using eq. 20 for the
4 seven meters was $135. \pm 4. \text{ Wm}^{-2}$ which compares well with the measured flux
5 density.

6 Figure 3 indicates how well the meter thermal conductivity, K_p , predicted
7 by eq. 15 using data from Tables 1,3 and 5 compares with the estimated conduc-
8 tivity of each meter listed in Table 3. Predicted values compare well with esti-
9 mates for four of the six meters. The predicted values of the other two meters,
10 REBS.#87049 and ETL.#16, however show large deviations from their estimated
11 conductivities of 14 and -25 percent, respectively. The thermal conductivity of
12 ETL.#16 was estimated using an electrical circuit analog of thermal resistances
13 of meter components and was not based on direct measurement. It is possible in
14 fact that the meter's epoxy filler contained gas bubbles which if taken into
15 account would have dropped the estimate of effective meter conductivity to a
16 value in closer agreement with the predicted value. The conductivity of
17 REBS.#87049 was overpredicted perhaps due to meter misalignment in the dry
18 sand medium. After the meter was calibrated, a check of its orientation revealed
19 that its upper face was not quite parallel with the heater plate. This could have
20 reduced the signal during calibration thus increasing C_1 and leading to an
21 inflated value of K_p .

22 Table 6 and Figure 3 show that the theory of steady heat conduction in
23 composite media can be applied usefully to heat flux meters embedded in porous
24 media, although exact agreement between theory and experimental results is not
25 expected for every meter because theory assumes that all meters are homogene-
26 ous and isotropically conducting ellipsoids, while in reality meters are composed
27 of materials with different conductivities and are usually flat in shape.

1 VI. Discussion

2 Check of media thermal conductivities

3 In an effort to substantiate the agreement between the heat flux density
4 measured in saturated glass beads and that predicted by eq. 20, we measured the
5 thermal conductivities of all three media using the transient line-source or
6 cylindrical probe method (DeVries and Peck,1958a&b). Media were tested in
7 the same room using the same media samples and water supply as were
8 employed using the steady-state method. The probe was similar in construction
9 to that described in Jackson and Taylor (1986, pp. 947-952). Using dry sand
10 and saturated glass bead media the results were in good agreement with those
11 obtained via steady-state. At an ambient temperature of 21 C we obtained a
12 mean value of $0.284 \pm 0.020 \text{ Wm}^{-1}\text{C}^{-1}$ for dry sand and a mean value of 0.745
13 $\pm 0.028 \text{ Wm}^{-1}\text{C}^{-1}$ for saturated glass beads. However, the mean value of $2.78 \pm$
14 $0.074 \text{ Wm}^{-1}\text{C}^{-1}$ obtained for saturated sand did not agree with the steady-state
15 value of $1.77 \text{ Wm}^{-1}\text{C}^{-1}$.

16 We have no explanation for why the probe method gave a mean value for
17 saturated sand that is 57 percent larger than that measured under steady condi-
18 tions. But values reported in the literature do tend to support this result. Using
19 a steady-state method Kersten (1949) found that the thermal conductivity of
20 nearly-saturated quartz sand was $2.01 \text{ Wm}^{-1}\text{C}^{-1}$. He also reported the results of
21 another group using the same sand near saturation. They determined a value of
22 $1.65 \text{ Wm}^{-1}\text{C}^{-1}$ also under steady conditions. On the other hand, using the tran-
23 sient method DeVries (1963) found that saturated quartz sand has a thermal con-
24 ductivity of $2.51 \text{ Wm}^{-1}\text{C}^{-1}$. Mogensen (1970) reported a value of 2.70 Wm^{-1}
25 C^{-1} for saturated sand using the same method. Thus, the values obtained using
26 the steady-state technique tend to agree with our steady-state value, while those
27 ~~acquired using the transient technique tend to agree with our transient value.~~

1 Until more direct comparisons between the two methods of obtaining thermal
2 conductivity of saturated sand are made, we see no reason to believe that our
3 steady-state value is incorrect.

4 Criteria for rejecting G_0

5 Equation 20 can be written in the form

$$6 \quad G_0 = \frac{\left[\frac{C_2 K_1 - C_1 K_2}{C_1 - C_2} \right] \cdot \frac{\Delta T}{\Delta z} \Big|_{\infty}}{1 + \epsilon} \quad (29)$$

7 where

$$8 \quad \epsilon = \frac{K_1 - K_2}{C_1 - C_2} \cdot \frac{\frac{\Delta T}{\Delta z} \Big|_{\infty}}{V_0} \quad (30)$$

9 If $\epsilon = -1$ then G_0 is undefined, but analysis shows this is unlikely except at
10 very high media thermal conductivities. The signs of the parameters in eq. 30
11 have been defined so that ϵ is always negative. We evaluated ϵ for all meters
12 used in the experiment and found that values for saturated glass beads ranged
13 from -9.5 for F.#64 to -2.4 for Th.#14 confirming that there was no serious error
14 in the computed values of G_0 for our choice of media and meters. As the ther-
15 mal conductivity of the test medium increases, however, ϵ for all meters asymp-
16 totically approaches -1. As a hypothetical example, consider the saturated sand
17 as a test medium. Taking corresponding data of $\Delta T/\Delta z \Big|_{\infty}$ and G_2 from Table 4
18 and C_2 from Table 5 we found that ϵ ranged from -4.3 for F.#64 to -1.6 for
19 Th.#14. Thus meters of low conductivity and low H such as Th.#14 are most
20 likely to cause error in G_0 in highly conductive media.

21 Unlike heat flow inside the calibration box, heat flow in field soils is rarely
22 as uniform or steady. Nonuniformity may cause ϵ to be positive when the heat
23 flux through the meter is opposite in direction to the flux in the soil at large hor-
24

1 horizontal distances from the meter, i.e. V_0 and $\Delta T/\Delta z|_{\infty}$ have the same sign. But
2 this should occur only briefly twice per day, once in the morning and again at
3 night when the heat flux is small at meter depths of 5 to 10 cm. During the
4 remainder of the day ϵ should be generally less than -1.

5 Each time ϵ shifts from negative to positive and back to negative again,
6 characteristic of unsteady soil heat flux, data of ϵ may lie in the neighborhood of
7 -1 yielding erroneous values of G_0 . This requires that we establish an interval
8 for ϵ around -1 for which G_0 is rejected. Considering the measurement uncer-
9 tainty associated with heat meters and thermocouples inserted into field soils we
10 propose a rejection interval of $-1.5 < \epsilon < -0.5$ with more appropriate values of G_0
11 substituted by interpolation, if necessary. Because a thick (low H) meter of low
12 conductivity surrounded by a highly conductive medium yields a value of ϵ
13 closest to -1 in a steady, uniform heat flow pattern, it is likely that in soils this
14 meter-medium combination will produce longer periods during the day when G_0
15 must be rejected. Therefore, thin meters with thermal conductivities exceeding
16 about $0.5 \text{ Wm}^{-1}\text{C}^{-1}$ should provide better estimates of G_0 .

17 **Effect of Temperature**

18 Under our laboratory conditions the temperature of the test medium
19 (saturated glass beads) was within $\pm 1 \text{ C}$ of the temperature of the two calibra-
20 tion media at meter depth. But the temperature of field soils may differ substan-
21 tially from that of the calibration media so we need to examine what effect this
22 could have on the accuracy of G_0 . The meter signal, V_0 , is the only parameter
23 in eq. 20 that depends upon the absolute soil temperature due to the temperature
24 response of the Seeback effect. Most heat-meters in use today are constructed of
25 a copper-constantan thermopile which exhibits a temperature response of the
26 Seeback effect of +2.5 percent per 10 C rise over the 0 C to 40 C range. For
27 example, if the soil temperature is 10 C higher than the temperature of the two

1 calibration media, then the meter signal will be 2.5 percent too large causing soil
2 heat flux density to be overestimated by 2.5 percent using direct calibrations.
3 Such error has been deemed negligibly small in comparison to much larger
4 errors inherent in the field use of direct calibration methods. However, for the
5 same temperature difference analysis using eq. 20 and data from Tables 4 and 5
6 for saturated glass beads shows that G_0 is overestimated by a greater percen-
7 tage, 2.9 percent for F.#64 to as much as 4.4 percent for Th.#14. If saturated
8 sand were the test medium, then percentage values are even greater, 3.2 and 7.2,
9 respectively.

10 Although we made no attempt to change the temperature of the test
11 medium in the lab to see whether this would affect our comparison of computed
12 heat flux densities, we did test the effect of temperature on direct meter calibra-
13 tions in our dry sand over a range from 25 C to 40 C and found that the average
14 calibration coefficient dropped by 2 percent per 10 C rise. This is consistent
15 with the temperature response of the Seeback effect of a Cu/Con thermopile.
16 One of the meters, ETL.#16, constructed of a Peltier cooler, a bismuth-telluride
17 semiconductor thermopile, also showed about -2 percent change per 10 C rise.
18 This agreed with test results by Weaver and Campbell (1985) in dry sand indi-
19 cating an average drop of 2.5 percent per 10 C using 21 Peltier coolers over a
20 range from 12 C to 36 C. We conclude that G_0 should be more sensitive to the
21 deviation of soil temperature from media calibration temperature than is soil heat
22 flux density computed from direct calibrations especially if employing thick
23 meters of low thermal conductivity in a highly conductive soil.

24 Contact Resistance

25 Based on the finding of Fuchs and Hadas (1973) that anodized aluminum-
26 plated meters, e.g. F.#64, are so constructed as to be virtually free of contact
27 ~~resistance with a coarse-textured sand, our experimental results indicate that~~

1 contact resistance was negligible for all meters tested in our dry, coarse quartz
2 sand. Comparison of heat flux densities in saturated glass beads using eq. 20
3 between those based on calibration data of F.#64 and those based on data of the
4 other meters with much less conductive exteriors showed no systematic
5 difference (Table 5). If there were substantial contact resistance in the dry sand
6 - low conductivity meter system, then the calibration coefficient, C_1 , should be
7 larger than if there were no contact resistance. This would imply via eq.20 that
8 the predicted flux density should be greater for such meters than for F.#64. This
9 is definitely not the case. Tests by Weaver and Campbell (1985) substantiate
10 our results. They found that covering meters of the Peltier cooler type with
11 aluminum foil reduced the meter calibration in dry sand by less than 5 percent.

12 **Application to Soils**

13 Application of eq. 20 rather than a direct calibration to compute soil heat
14 flux density requires an additional calibration in a second medium and a meas-
15 urement of soil temperature gradient in the direction of heat flow at meter depth.
16 Considering that soils usually exhibit lateral spatial variability in heat flow we
17 suggest that the temperature gradient be measured at a distance of 3 to 6 cm
18 away from the meter.

19 To achieve an areal average soil heat flux using direct calibration research-
20 ers often connect meters placed at a uniform depth in series and compute the
21 overall calibration coefficient as

$$22 \quad C = \left\{ \sum_i \frac{1}{C_i} \right\}^{-1} \quad (31)$$

23 where C_i is a calibration coefficient for the i -th meter. Use of eq. 20 with
24 series-connected meters will require the same coefficients for all meters in each
25 calibration medium. The voltage, V_0 , is then equal to the total voltage signal
26
27

1 divided by the number of meters in series.

2 In studies of the ground surface energy budget the method described by eq.
3 20 could easily be adapted to the estimation of soil surface heat flux density.
4 Several temperature measurements in the soil layer between the surface and
5 meter depth are required for calorimetric estimates when heat flux meters are
6 buried between 5 and 10 cm deep. This range of placement depths should be
7 adequate based on the maximum theoretical size of the region of heat flux per-
8 turbation around the meters tested in our experiment. An additional temperature
9 measurement 1 or 2 cm below meter depth would serve to provide $\Delta T/\Delta z |_{\infty}$.

10 Some problems cannot be eliminated with the use of eq. 20. The meter
11 signal may be inadequate because of misalignment of the meter in the soil or
12 because of air pockets between the meter and the soil matrix. The meters
13 respond only to the sensible heat component of the energy flux through soil;
14 however, the latent heat flux component may be substantial in warm, moist soils
15 and is often pointed opposite to the direction of the sensible heat component so
16 that the meter may be overestimating the total energy flux through the soil under
17 these conditions. This is further complicated by the fact that meters are impervi-
18 ous to the flux of water vapor so that vapor may condense on them falsely modi-
19 fying the meter signal. This problem can be minimized by reducing the size of
20 the meter (Fuchs,1986).

21 VII. Conclusions

22 In this paper the theory of heat-flux meters has been tested and confirmed
23 under steady-state laboratory conditions. From the theory we derived eq. 20 for
24 determining the heat flux density in porous media and showed that it is more
25 accurate than direct calibration equations. We believe the results for saturated
26 glass beads medium are applicable in fine to coarse-textured soil media where

27 the thermal environment is approximately steady-state at least 5 cm below the

1 soil surface. This in turn should serve to provide for more accurate assessment
2 of the energy budget of land surfaces.

3 The following set of conditions summarize proper meter design and calibra-
4 tion for evaluating G_0 in soils. The first three conditions correspond to those
5 listed by Philip (1961) for evaluating soil heat flux density by direct calibration.

- 6 1. The meter should be made thin ($H > 0.65$).
- 7 2. The meter should be calibrated in two porous media with thermal conduc-
8 tivities representing the opposite extremes of the soil in which the meter is
9 to be buried. For mineral soils dry and water-saturated sand are con-
10 venient.
- 11 3. The thermal conductivity of the meter should be high, at least $0.5 \text{ Wm}^{-1}\text{C}^{-1}$
12 for mineral soils.
- 13 4. The meter should be calibrated at the mean temperature of the soil in which
14 it is to be exposed.

15
16 **Acknowledgements:**

17 We gratefully acknowledge the funding support of NASA as part of the
18 First ISLSCP Field Experiment (NAG 5-389). We thank Mr. Roy Theisen and
19 Mr. Dale Reed for their technical assistance during the construction and testing
20 of the calibration apparatus. We also thank Dr. J.B. Sisson for the use of his
21 thermal conductivity probe.
22
23
24
25
26
27

1 **References:**

2 Biscoe,P.V.,R.A. Saffell and P.D. Smith. 1977. An apparatus for calibrating soil
3 heat flux plates. *Agr. Meteorol.* 18:49-54.

4 Carslaw,H.S. and J.C. Jaeger. 1959. *Conduction of Heat in Solids.* 2nd ed.
5 Clarendon Press, Oxford, England, 510pp.

6 De Vries,D.A. 1963. Thermal properties of soils. Chapter 7 in: *Physics of the*
7 *Plant Environment.* W.R. Van Wijk (ed.), John Wiley and Sons,Inc.,NY.
8 382 pp.

9 De Vries,D.A. and A.J. Peck. 1958a. On the cylindrical probe method of
10 measuring thermal conductivity with special reference to soils, Part I. *Aust.*
11 *J. Phys.* 11:255-271.

12 De Vries,D.A. and A.J. Peck. 1958b. On the cylindrical probe method of
13 measuring thermal conductivity with special reference to soils, Part II. *Aust.*
14 *J. Phys.* 11:409-423.

15 Fuchs,M. 1986. Heat flux. Chapter 40 in: *Methods of Soil Analysis, Part 1. Phy-*
16 *sical and Mineralogical Methods, Agron. Mono. No. 9 (2nd ed.).*

17 Fuchs,M. and C.B. Tanner. 1968. Calibration and field test of soil heat flux
18 plates. *Soil Sci. Soc. Am. Proc.* 32:326-328.

19 Fuchs,M. and A. Hadas. 1973. Analysis of the performance of an improved soil
20 heat flux transducer. *Soil Sci. Soc. Am. Proc.* 37:173-175.

21 Jackson,R.D. and S.A. Taylor. 1986. Thermal conductivity and diffusivity.
22 Chapter 39 in: *Methods of Soil Analysis, Part 1. Physical and Mineralogical*
23 *Methods, Agron. Mono. No. 9 (2nd ed.).*

24 Kersten,M.S. 1949. Thermal properties of soils. *Univ. of Minnesota, Eng. Exp.*
25 *Stn. Bull. No. 28.* 227pp.
26

27

1
2
3
4
5
6
7
8
9
10
11
12
13
14
15
16
17
18
19
20
21
22
23
24
25
26
27

Kimball,B.A. and R.D. Jackson. 1979. Soil heat flux. Chapter 3.4 in:
Modification of the Aerial Environment of Crops,pp.211-229, B.J. Barfield
and J.F. Gerber (Eds.), Am. Soc. Agr. Eng. Mono. 2, St. Joseph, MO.
538pp.

Mogensen,V.O. 1970. The calibration factor of heat flux meters in relation to the
thermal conductivity of the surrounding medium. Agr. Meteorol. 7:401-410.

Philip,J.R. 1961. The theory of heat flux meters. J. Geophys. Res. 66:571-579.

Weaver,H.L. and G.S. Campbell. 1985. Use of Peltier coolers as soil heat flux
transducers. Soil Sci. Soc. Am. J. 49:1065-1067.

Table 1. Composition of media, power applied to calibration box, power loss through insulation, and derived thermal conductivity (K) of media.

Medium	Particle Size (mm)	Porosity (%)	Applied Power (watts)	Power Loss (watts)	K ($\text{Wm}^{-1}\text{C}^{-1}$)
Sand, dry quartz	0.5-1.0	38	9.58	2.78	0.274
Glass beads, water-saturated, spherical	0.425-0.600	39	15.09	2.55	0.708
Sand, water-saturated quartz	0.5-1.0	38	18.30	2.54	1.77

Table 2. Distance from center of meter along x and z-axes to where $P(x,z)$ is $\pm 3\%$ for two, opposite extreme cases.

Parameter	Case (i)	Case (ii)
Meter	REBS. 85020*	ETL 16*
Meter thickness (mm)	5.1	6.8
Length of side (mm)	32.3	34.7
Geometrical factor, H	0.741	0.691
Meter conductivity ($Wm^{-1}C^{-1}$)	0.48**	1.7**
Medium conductivity ($Wm^{-1}C^{-1}$)	1.77	0.274
Distance to $P(x,z) = \pm 3\%$:		
along z-axis (mm), from eq. 24	32.	33.
along x-axis (mm), from eq. 25	32.	33.

* Manufactured by (i) Radiation Energy Balance Systems, Inc. and (ii) our lab, respectively.

** Manufacturers' estimates based on component thermal conductivities.

Table 3. Meter identification, shape, size, associated oblate spheroid shape factor (H) and estimated thermal conductivity (K_p).

Meter	Shape	Dimensions (mm)	H	K_p ($Wm^{-1}C^{-1}$)
REBS. 85020	Square	32x32x5.1	0.741	0.48
ETL. 16	Square	34x36x6.8	0.691	1.7
Th. 14	Disc	25.6 dia.; 2.84 thick	0.785	0.335
F.64	Rectangle	30x80x2.8	-	-
REBS. 87049	Square	32x32x5.1	0.738	0.995
REBS. 85017	Square	32x32x5.1	0.741	0.48
REBS. 87054	Square	33x33x5.1	0.745	0.995

Abbrevs: REBS. = Radiation Energy Balance Systems, Inc., Seattle, WA
 ETL = Evapotranspiration Lab, Kansas State Univ., Manhattan, KS
 Th. = C. W. Thornthwaite Associates, Elmer, NJ
 F. = Dr. Marcel Fuchs, Agric. Res. Org., Israel

Table 4. Heat flux density (G), temperature difference (ΔT) across the depth of medium (ΔZ) and derived temperature gradient ($\Delta T/\Delta Z|_{\infty}$) for the three media.

Medium	G (Wm^{-2})	ΔT (C)	ΔZ (m)	$\Delta T/\Delta Z _{\infty}$ (Cm^{-1})
Dry sand	72.4	-19.8	0.075	-264.
Saturated glass beads	133.	-14.5	0.077	-188.
Saturated sand	168.	- 7.2	0.076	- 94.7

Table 5. Meter calibration coefficients in dry sand (C_1) and in saturated sand (C_2), meter signal (V_o) and heat flux density in saturated glass beads (G_o) predicted from eq. 20.

Meter	C_1	C_2	V_o	G_o
	$(Wm^{-2}mV^{-1})$	$(Wm^{-2}mV^{-1})$	(mV)	(Wm^{-2})
	7.8	34.8	6.06	140.
	.9	29.4	5.77	130.
	.	414.	0.523	133.
	.	139.	1.10	132.
	.5	46.6	3.67	135.
	.1	42.3	4.88	138.
	.8	46.3	3.82	135.

Table 6. Predicted heat flux densities in saturated glass beads using direct calibration in dry sand ($G_1 = C_1 V_0$), saturated sand ($G_2 = C_2 V_0$) and using eq. 20 (G_0):

Meter	G_1 (Wm^{-2}) (%)	G_2 (Wm^{-2}) (%)	G_0 (Wm^{-2}) (%)
REBS. 85020	108. (-19.)	211. (+58.)	140. (+5.)
ETL. 16	115. (-14.)	169. (+27.)	130. (-3.)
TH. 14	99. (-26.)	216. (+62.)	133. (-0.)
F. 64	124. (-7.)	152. (+14.)	132. (-1.)
REBS. 87049	119. (-10.)	171. (+28.)	135. (+1.)
REBS. 85017	108. (-19.)	206. (+55.)	138. (+4.)
REBS. 87054	118. (-12.)	177. (+33.)	135. (+1.)

Values in parentheses represent percentage deviation from measured heat flux density.

Figure Captions:

Figure 1. Vertical cross-section through center of calibration box with location of thermocouple junctions marked by x's.

Figure 2. Vertical cross-section through center of an oblate spheroid depicting conceptual isotherms (dashed lines) for $K > K_p$.

Figure 3. Predicted versus estimated thermal conductivity of heat-flux meters.

1
2
3
4
5
6
7
8
9
10
11
12
13
14
15
16
17
18
19
20
21
22
23
24
25
26
27

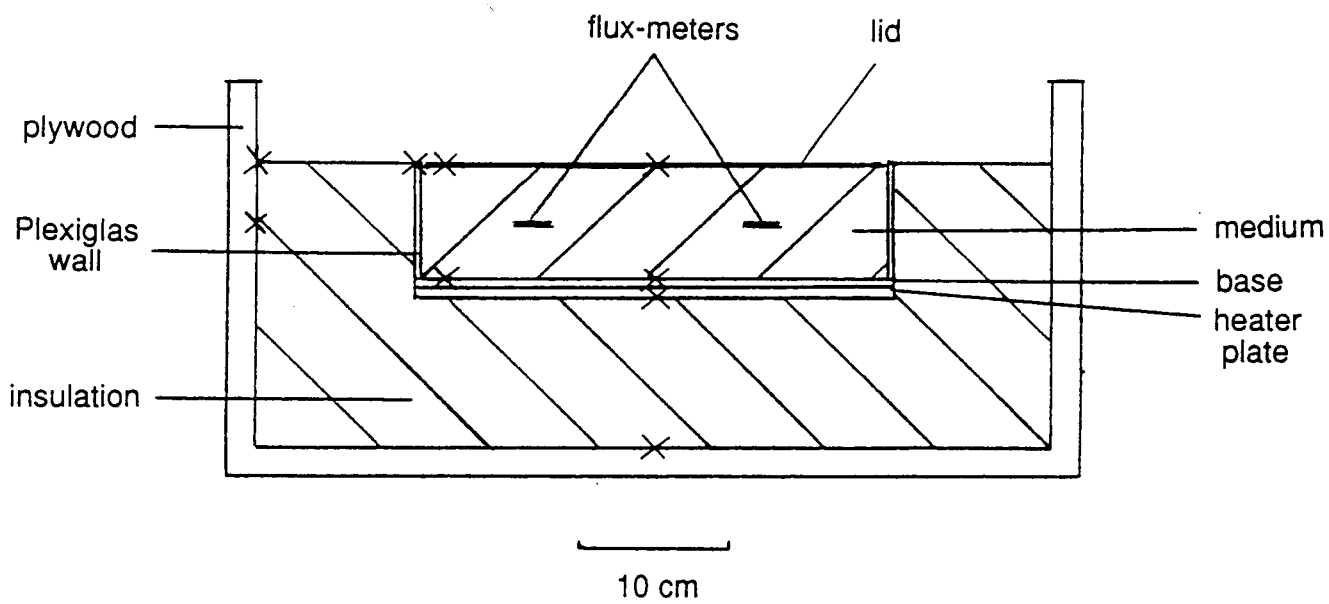


Fig. 1.

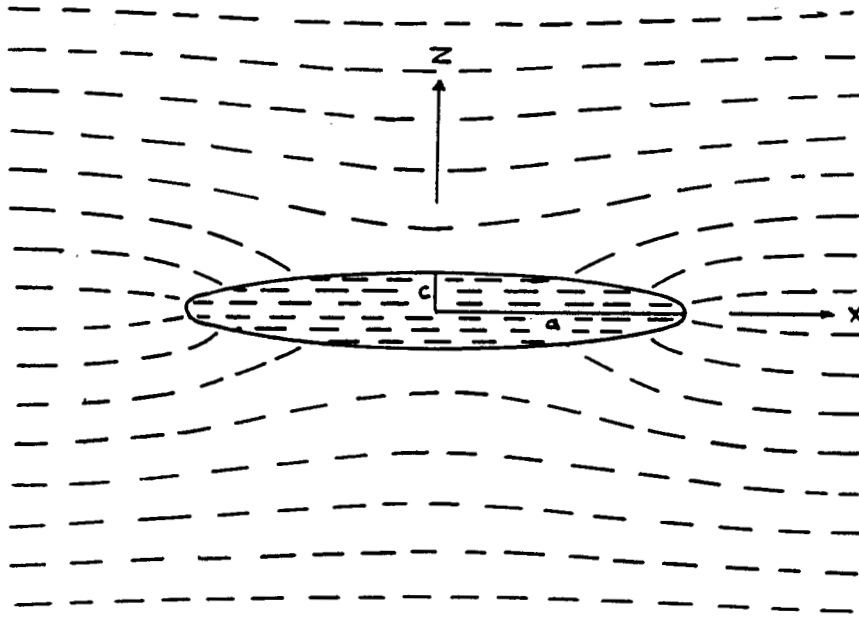


Fig. 2

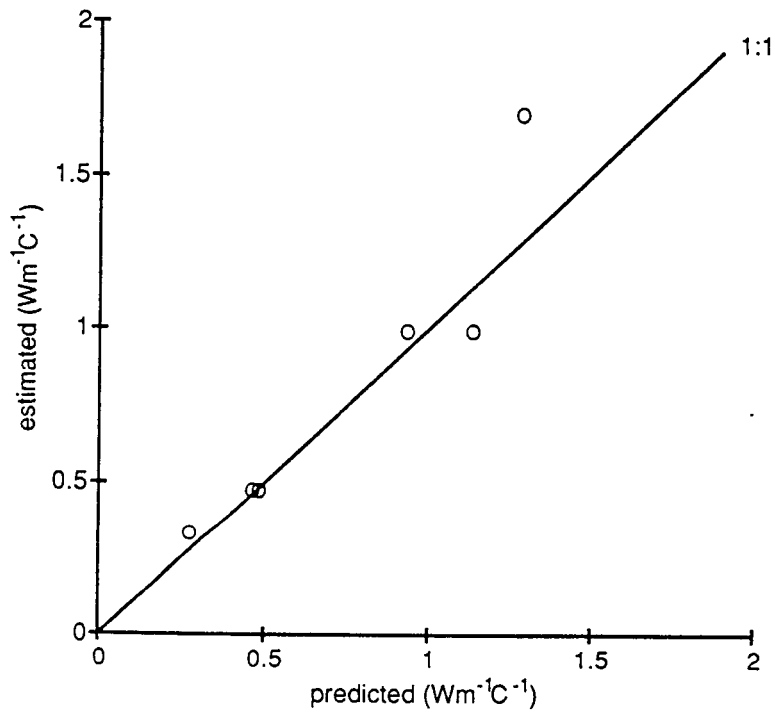


Fig. 3

Chapter 5

Soil Water Content Versus Water Potential for FIFE Sites



125 YEARS

KANSAS
STATE
UNIVERSITY

January 17, 1989

Department of Agronomy
Crop, Soil, and
Range Sciences
Throckmorton Hall
Kansas State University
Manhattan, Kansas 66506
913-532-6101

Ed Kanemasu
E.T. Lab
Waters Hall
CAMPUS

Dear Ed:

In conjunction with the NASA-FIFE Project, the following moisture release values were obtained (*By volume*).

site #	20 cm			30 cm			40 cm		
	Sat.	1/3-bar	15-bar	Sat.	1/3-bar	15-bar	Sat.	1/3-bar	15-bar
1	0.398	0.239	0.162	0.431	0.329	0.281	0.383	0.297	0.256
2	0.410	0.277	0.213	0.452	0.364	0.322	0.444	0.329	0.274
3	0.404	0.275	0.213	0.428	0.348	0.310	0.407	0.313	0.268
4	0.424	0.267	0.192	0.409	0.348	0.319	0.398	0.325	0.291
5	0.396	0.248	0.177	0.453	0.358	0.313	0.393	0.276	0.219
9	0.386	0.248	0.182	0.434	0.353	0.314	0.407	0.334	0.298
10	0.301	0.157	0.087	0.158	0.152	0.149	0.343	0.288	0.262
11	---	---	---	---	---	---	---	---	---
13	0.383	0.256	0.195	0.422	0.334	0.292	0.395	0.309	0.267
15	0.365	0.224	0.157	0.421	0.315	0.264	0.422	0.294	0.233
17	0.378	0.248	0.186	0.385	0.321	0.291	0.362	0.302	0.273
19	0.303	0.200	0.151	0.365	0.315	0.292	0.412	0.318	0.273
20	0.370	0.246	0.187	0.379	0.308	0.274	0.346	0.272	0.236
21	0.371	0.234	0.169	0.393	0.337	0.310	0.394	0.322	0.287
23	0.387	0.248	0.182	0.387	0.321	0.290	0.358	0.304	0.278
28	0.398	0.252	0.182	0.422	0.351	0.316	0.415	0.344	0.310
29	0.380	0.241	0.174	0.420	0.334	0.293	0.367	0.292	0.256
36	0.384	0.243	0.176	0.413	0.338	0.302	0.392	0.312	0.274
38	0.383	0.256	0.194	0.411	0.336	0.300	0.413	0.310	0.261

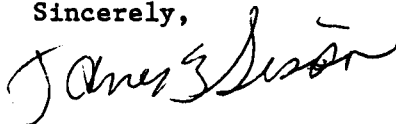
The data was generated from pressure plate and thermal couple psychrometer data.

Page 2
Ed Kanemasu
January 17, 1989

We did not do Site 11 as Dr. Shashi Verma was the principal investigator at that site.

If you have any questions, please feel free to contact me.

Sincerely,



J. B. Sisson
Assistant Professor

nkW

Chapter 6

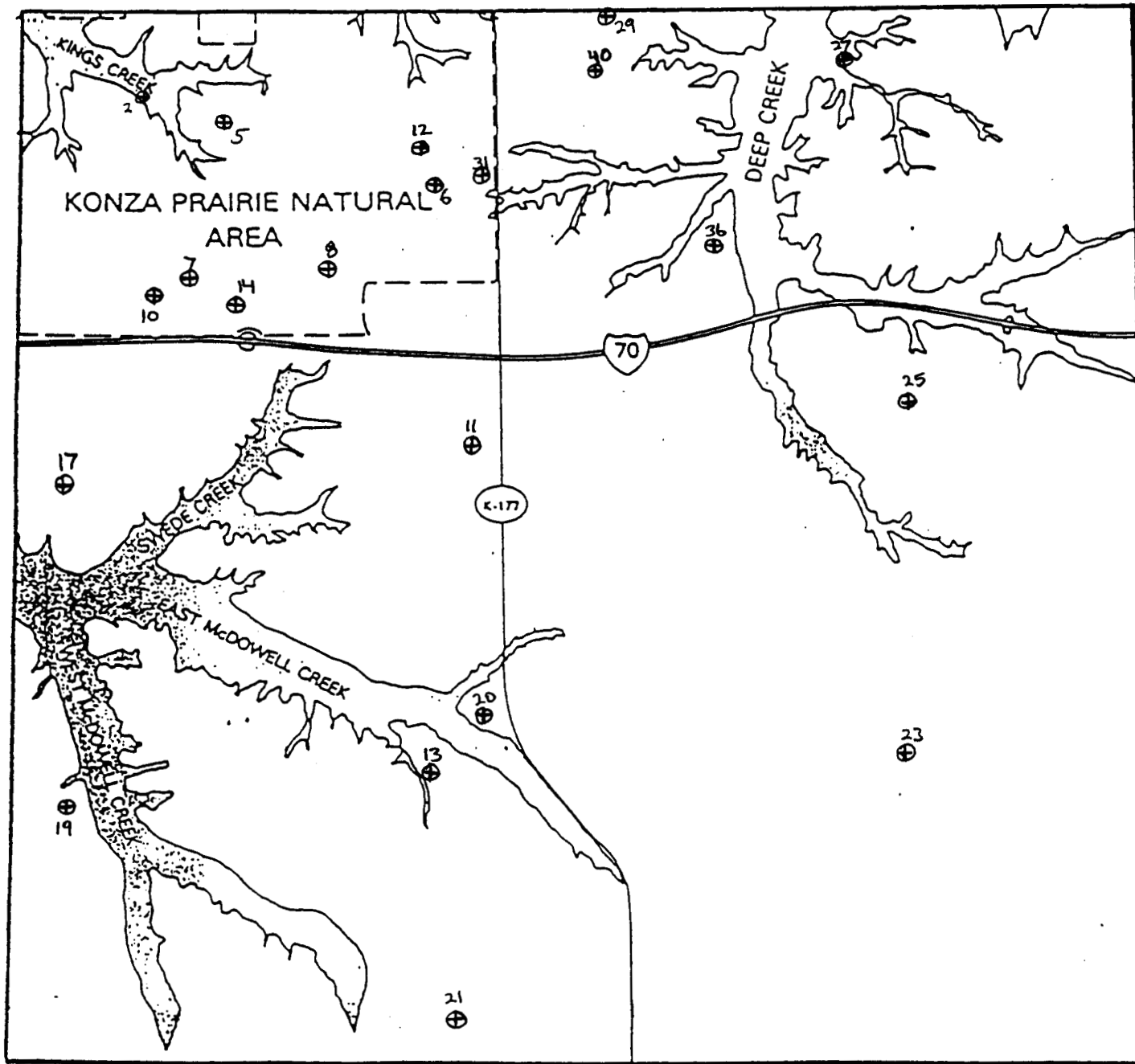
1988 Plant and Soil Data for FIFE Sites

The FIFE plant and soil sample monitoring program for 1988 was conducted from April 11 (102 Julian) - October 25 (299 Julian) at 21 sites. Figures A and B contain geographic location and treatment information, respectively, for the sites.

Six, .1 m² plant samples were randomly collected, biweekly, along 60° radials progressing clockwise from North and between 25 - 60 m from the center of each site location. Samples were analyzed for biomass and leaf area and the data is summarized on pages ? - ?. Values represent means of all six samples with zeros indicating that no data was available for that sample/station.

Five volumetric soil samples were collected weekly at random locations in the center and approximately 30 meters north, west, south and east of each site. 0-5, 5-10 and 0-10 cm soil moisture data is summarized on pages ? - ?. Zeros indicate absence of data.

Neutron moisture readings were collected within 48 hours of gravimetric samples at sites where the geography permitted installation of neutron tubes (11 sites). Mm of water mean values for each tube and station are summarized on pages ? - ?. Zeros indicate absence of data.



15 km

15 km

1988 FIFE SITES
Location & Treatment Information

STN #	NAME	SLOPE	ASPECT	TX	ELEV	USGS MAP	No 'ng	E 'ng	N. Lat	W. Long	Grazed	Phone	Owner
2	BR/DU	2°	N	U	345m	Swede	43,30,410	07,08,225	39 06 00	96 35 30	N	9-1961	Konza
5	SPAM1	1°	Top	U	405m	Swede	43,29,805	07,09,512	39 05 39	96 34 39	N	9-1961	Konza
6	BR/DS	14°	S	U	439m	Swede	43,29,854	07,12,366	39 05 37	96 32 39	N	9-1961	Konza
7	PAM2	11°	NW	B	410m	Swede	43,28,000	07,09,250	39 04 40	96 34 52	N	9-1961	Konza
8	BR/DB	5°	SE	B	433m	Swede	43,27,780	07,10,683	39 04 33	96 03 53	N	9-1961	Konza
10	BR/DW	13°	W	U	420m	Swede	43,27,463	07,08,463	39 04 24	96 35 25	N	9-1961	Konza
11(44)	PAM7	2°	N	B	445m	Swede	43,25,230	07,12,730	39 03 07	96 32 30	N	539-8090	G. Poole
12	BR/DN	20°	N	U	425m	Swede	43,30,195	07,11,927	39 05 49	96 32 58	N	9-1961	Konza
13(42)	PAM3	1°	Rot	U	385m	Swede	43,20,500	07,12,150	39 05 35	96 32 59	G	776-8458	B. Gehrt
14	BR/DE	12°	E	U	420m	Swede	43,27,244	07,06,850	39 04 15	96 34 39	N	9-1961	Konza
17	PAM6	3°	SE	U	390m	Swede	43,24,960	07,06,850	39 03 02	96 35 53	G	776-4963	M. Potter
19	PAM8	2°	N	U	385m	Swede	43,20,230	07,07,270	39 00 29	96 36 23	G	539-5870	J. Poole
20	BR/L6	4°	SW	B	410m	Swede	43,21,500	07,13,000	39 01 08	96 31 03	N	539-5870	J. Poole
21	SPAN9	1°	Top	U	440m	White							
23	PAM10	3°	NE	B	440m	City	43,16,700	07,12,770	38 58 30	96 32 38	G	762-5086	R. Glessner
25(34)	PAM	1°	Top	B	420m	Wamego	43,21,150	07,18,850	39 00 52	96 28 21	G	357-4441	K.D.L.C.
27	PAM5	18°	W	U	366m	Wamego	43,25,630	07,18,500	39 03 23	96 28 22	G	776-5171	P. Gehrt
29	SPAM	1°	Top	B	415m	Swede	43,31,100	07,17,610	39 06 13	96 29 01	G	776-5255	F. Rudolph
31	PAM4	3°	W	U	385m	Swede	43,32,330	07,14,420	39 06 54	96 31 12	G	776-8458	B. Gehrt
34(25)	BR/L5	1°	Top	B	420m	Wamego	43,25,850	07,12,780	39 05 36	96 32 23	N	9-1961	Konza
36	BR/L4	4°	E	U	365m	Swede	43,25,630	07,18,500	39 03 23	96 28 22	G	776-5171	P. Gehrt
40	BR/L1	12°	S	B	410m	Swede	43,28,675	07,16,50	39 04 55	96 30 10	G	776-6643	C. Barry
42(13)	BR/L2	1°	Bot	U	385m	Swede	43,31,625	07,14,200	39 06 30	96 31 21	G	776-8458	B. Gehrt
44(11)	BR/L3	2°	N	B	445m	Swede	43,20,500	07,12,150	39 05 34	96 32 59	G	776-8458	B. Gehrt
							43,25,230	07,12,730	39 03 07	96 32 30	N	539-8090	G. Poole

DU = Dave's Unburned
DB = Dave's Burned
DN = Dalin's North
DS = Dalin's South
DE = Dalin's East
DW = Dalin's West

L = Leo Fritschen

Day of Year	Station	[-- Fresh Weight ---]			[--- Dry Weight ----]			[----- LAI -----]		
		Total Grass	Non-Grass		Total Grass	Non-Grass		Total Grass	Non-Grass	
		[----- g/m2 -----]						[----- m2/m2 -----]		
116	2	385	385	0	133	133	0	0.79	0.79	0.00
126	2	522	522	0	174	174	0	1.09	1.09	0.00
134	2	616	616	0	234	234	0	1.36	1.36	0.00
140	2	593	586	7	215	212	3	1.44	1.43	0.01
146	2	653	638	15	240	236	4	1.73	1.71	0.02
153	2	894	891	2	319	319	0	2.31	2.30	0.00
165	2	445	445	0	230	230	0	1.02	1.02	0.00
167	2	628	621	7	254	251	3	1.33	1.32	0.01
181	2	355	335	21	198	192	6	0.77	0.73	0.04
195	2	281	275	6	157	155	2	0.72	0.71	0.01
209	2	351	348	3	202	201	1	0.83	0.83	0.00
223	2	393	388	5	184	182	2	0.73	0.72	0.01
238	2	315	230	85	146	121	25	0.53	0.48	0.06
260	2	257	241	16	116	109	6	0.49	0.47	0.02
281	2	274	262	11	96	91	4	0.73	0.72	0.01

Day of Year	Station	[-- Fresh Weight ---]			[--- Dry Weight ----]			[----- LAI -----]		
		Total Grass	Non-Grass		Total Grass	Non-Grass		Total Grass	Non-Grass	
		[----- g/m2 -----]						[----- m2/m2 -----]		
110	5	12	10	2	8	7	1	0.03	0.02	0.00
127	5	23	23	0	16	15	0	0.06	0.06	0.00
139	5	116	97	19	46	42	4	0.15	0.13	0.02
153	5	794	643	151	224	181	43	1.55	1.33	0.22
167	5	627	571	56	197	177	19	1.20	1.12	0.08
181	5	360	225	136	179	129	50	0.66	0.44	0.22
195	5	411	352	59	221	190	31	0.84	0.77	0.07
209	5	564	532	32	289	273	17	1.16	1.11	0.05
223	5	732	610	123	325	277	48	1.17	1.00	0.17
237	5	535	500	35	245	231	14	0.90	0.85	0.05
264	5	292	238	54	135	112	23	0.39	0.32	0.06
280	5	211	157	54	105	80	25	0.26	0.21	0.05

Day of Year	Station	[-- Fresh Weight ---]			[--- Dry Weight ----]			[----- LAI -----]		
		Total Grass	Non-Grass		Total Grass	Non-Grass		Total Grass	Non-Grass	
		[----- g/m2 -----]						[----- m2/m2 -----]		
125	6	75	58	17	17	14	4	0.10	0.08	0.02
145	6	433	297	136	158	104	54	0.64	0.49	0.15
161	6	540	286	254	209	137	73	1.02	0.52	0.50
175	6	369	247	122	202	142	60	0.57	0.41	0.16
190	6	419	369	51	190	173	17	0.96	0.84	0.12
203	6	802	448	354	371	200	171	1.54	1.00	0.53
217	6	588	537	50	290	263	26	0.92	0.81	0.11
231	6	645	258	387	313	140	173	0.86	0.33	0.53
252	6	309	181	129	183	108	76	0.38	0.23	0.15
277	6	234	196	38	130	109	20	0.23	0.20	0.03
295	6	94	77	16	60	50	10	0.11	0.09	0.02

Day of Year	Station	[-- Fresh Weight ---]		[--- Dry Weight ----]		[----- LAI -----]				
		Total Grass	Non-Grass	Total Grass	Non-Grass	Total Grass	Non-Grass			
		[----- g/m2 -----]						[----- m2/m2 -----]		
110	7	0	0	0	0	0	0	0.00	0.00	0.00
124	7	43	33	10	11	8	3	0.05	0.04	0.02
138	7	152	106	46	48	34	13	0.27	0.20	0.07
152	7	363	304	59	122	101	20	0.69	0.55	0.14
166	7	545	267	278	192	103	89	1.15	0.54	0.61
180	7	459	366	93	219	173	46	0.90	0.63	0.27
194	7	623	381	242	245	149	95	1.38	0.92	0.46
208	7	673	534	139	295	221	74	1.54	1.16	0.37
222	7	547	431	115	215	175	40	0.90	0.73	0.17
237	7	722	295	427	321	134	187	1.05	0.48	0.56
259	7	360	338	21	169	160	9	0.54	0.51	0.03
279	7	313	245	67	146	114	32	0.48	0.40	0.08

Day of Year	Station	[-- Fresh Weight ---]		[--- Dry Weight ----]		[----- LAI -----]				
		Total Grass	Non-Grass	Total Grass	Non-Grass	Total Grass	Non-Grass			
		[----- g/m2 -----]						[----- m2/m2 -----]		
110	8	0	0	0	0	0	0	0.00	0.00	0.00
126	8	107	97	10	30	28	2	0.20	0.18	0.02
134	8	224	185	38	65	57	8	0.41	0.35	0.06
140	8	285	262	23	99	92	8	0.62	0.57	0.05
146	8	341	287	54	114	98	16	0.76	0.68	0.08
153	8	429	392	36	147	136	11	1.03	0.97	0.07
165	8	419	377	41	182	168	14	0.87	0.79	0.08
167	8	355	338	16	150	143	7	0.78	0.75	0.02
181	8	361	257	104	185	144	41	0.65	0.49	0.16
195	8	479	449	30	199	186	13	1.25	1.18	0.07
209	8	611	593	19	306	297	8	1.37	1.34	0.03
223	8	470	438	32	244	230	14	0.78	0.72	0.06
238	8	465	456	9	239	235	4	0.79	0.79	0.01
260	8	382	355	27	163	151	11	0.69	0.67	0.02
284	8	328	296	32	147	133	14	0.58	0.55	0.03

Day of Year	Station	[-- Fresh Weight ---]		[--- Dry Weight ----]		[----- LAI -----]				
		Total Grass	Non-Grass	Total Grass	Non-Grass	Total Grass	Non-Grass			
		[----- g/m2 -----]						[----- m2/m2 -----]		
125	10	19	9	10	5	3	2	0.03	0.01	0.01
147	10	563	96	467	213	43	170	0.65	0.17	0.48
162	10	360	275	85	150	118	32	0.67	0.54	0.13
176	10	381	179	203	187	99	89	0.84	0.50	0.34
193	10	857	575	282	298	193	104	2.04	1.33	0.71
204	10	893	342	551	324	142	182	1.80	0.72	1.08
218	10	630	453	177	267	192	75	0.99	0.77	0.22
232	10	394	273	121	172	116	56	0.70	0.46	0.24
253	10	522	278	244	282	151	131	0.53	0.32	0.21
274	10	285	174	112	125	71	54	0.40	0.27	0.12
299	10	157	13	144	95	9	86	0.03	0.01	0.02

Day of Year	Station	[-- Fresh Weight ---]		[--- Dry Weight ----]		[----- LAI -----]				
		Total	Grass	Non-Grass	Total	Grass	Non-Grass	Total	Grass	Non-Grass
		[----- g/m2 -----]						[----- m2/m2 -----]		
110	11	0	0	0	0	0	0	0.00	0.00	0.00
124	11	104	100	4	32	31	1	0.18	0.17	0.01
138	11	356	304	53	108	95	13	0.70	0.62	0.08
152	11	650	610	41	203	193	10	1.51	1.44	0.07
166	11	521	451	70	199	176	23	1.18	1.07	0.11
180	11	1029	377	651	334	193	141	1.68	0.69	0.99
194	11	739	566	174	312	247	64	1.84	1.44	0.40
208	11	569	538	30	283	269	14	1.17	1.12	0.04
222	11	511	474	37	236	222	14	0.84	0.79	0.06
236	11	631	525	105	252	211	41	1.41	1.24	0.17
257	11	195	183	12	129	122	7	0.21	0.19	0.02
278	11	217	187	30	127	110	17	0.30	0.27	0.03

Day of Year	Station	[-- Fresh Weight ---]		[--- Dry Weight ----]		[----- LAI -----]				
		Total	Grass	Non-Grass	Total	Grass	Non-Grass	Total	Grass	Non-Grass
		[----- g/m2 -----]						[----- m2/m2 -----]		
125	12	74	24	50	20	7	13	0.11	0.04	0.07
145	12	248	186	62	69	52	17	0.45	0.32	0.12
161	12	395	241	153	158	105	53	0.89	0.54	0.34
175	12	458	363	95	211	178	33	0.90	0.71	0.19
190	12	758	266	492	361	115	246	1.46	0.55	0.90
203	12	398	270	127	181	124	57	0.90	0.64	0.26
217	12	625	290	335	332	145	188	1.05	0.55	0.50
231	12	542	270	272	267	133	134	0.83	0.49	0.34
250	12	544	216	329	308	130	178	0.71	0.33	0.38
277	12	201	160	41	118	91	27	0.18	0.16	0.03
295	12	30	11	19	15	5	10	0.04	0.02	0.02

Day of Year	Station	[-- Fresh Weight ---]		[--- Dry Weight ----]		[----- LAI -----]				
		Total	Grass	Non-Grass	Total	Grass	Non-Grass	Total	Grass	Non-Grass
		[----- g/m2 -----]						[----- m2/m2 -----]		
117	13	69	23	46	29	10	20	0.14	0.07	0.07
132	13	115	53	62	44	23	21	0.14	0.08	0.06
141	13	153	75	78	64	42	22	0.17	0.07	0.10
155	13	742	85	656	179	43	135	0.87	0.12	0.76
169	13	265	153	111	119	80	40	0.40	0.20	0.20
187	13	183	83	100	76	43	32	0.38	0.16	0.22
197	13	694	152	542	236	73	163	1.35	0.37	0.98
211	13	648	270	378	259	132	127	1.28	0.54	0.73
225	13	1008	160	848	406	92	314	1.22	0.21	1.01
242	13	490	187	303	231	110	121	0.58	0.22	0.36
265	13	760	112	647	337	57	280	0.72	0.16	0.56
285	13	339	173	166	164	88	77	0.31	0.19	0.12

Day of Year	Station	[-- Fresh Weight ---]		[--- Dry Weight ----]		[----- LAI -----]				
		Total Grass	Non-Grass	Total Grass	Non-Grass	Total Grass	Non-Grass			
		[----- g/m2 -----]				[----- m2/m2 -----]				
125	14	84	55	29	21	16	5	0.10	0.07	0.03
147	14	326	201	125	104	65	39	0.51	0.30	0.21
162	14	455	350	106	185	150	35	0.83	0.66	0.17
176	14	431	204	227	216	114	102	0.88	0.39	0.49
193	14	763	319	444	305	132	173	1.55	0.73	0.82
204	14	371	305	66	161	135	26	0.82	0.71	0.10
218	14	764	538	226	344	240	104	1.34	0.94	0.40
232	14	443	351	92	191	148	43	0.83	0.65	0.18
252	14	302	178	124	160	95	66	0.44	0.29	0.14
274	14	290	153	137	134	67	67	0.38	0.24	0.14
299	14	71	24	47	43	16	27	0.07	0.02	0.05

Day of Year	Station	[-- Fresh Weight ---]		[--- Dry Weight ----]		[----- LAI -----]				
		Total Grass	Non-Grass	Total Grass	Non-Grass	Total Grass	Non-Grass			
		[----- g/m2 -----]				[----- m2/m2 -----]				
111	17	38	9	29	23	5	17	0.04	0.02	0.02
130	17	309	65	243	155	29	126	0.51	0.10	0.41
140	17	198	138	59	76	59	18	0.28	0.21	0.07
155	17	391	262	128	138	102	36	0.62	0.47	0.14
169	17	600	233	367	249	108	142	0.86	0.34	0.52
183	17	290	163	127	111	67	45	0.59	0.38	0.21
197	17	375	271	104	173	129	43	0.79	0.61	0.19
211	17	329	250	79	190	147	43	0.61	0.51	0.10
225	17	396	112	284	239	66	173	0.40	0.17	0.23
243	17	134	107	28	86	69	17	0.18	0.13	0.05
266	17	188	96	92	112	57	55	0.20	0.10	0.10
288	17	57	35	22	31	22	8	0.07	0.05	0.02

Day of Year	Station	[-- Fresh Weight ---]		[--- Dry Weight ----]		[----- LAI -----]				
		Total Grass	Non-Grass	Total Grass	Non-Grass	Total Grass	Non-Grass			
		[----- g/m2 -----]				[----- m2/m2 -----]				
111	19	20	12	8	12	8	4	0.03	0.02	0.01
130	19	202	89	113	77	36	41	0.33	0.15	0.18
140	19	252	230	22	103	94	9	0.44	0.41	0.03
155	19	789	472	317	250	166	84	1.60	1.02	0.58
169	19	773	348	425	344	170	173	1.32	0.64	0.68
183	19	605	379	226	251	143	108	1.39	1.06	0.33
197	19	477	407	69	207	179	28	1.15	1.00	0.15
211	19	409	338	71	215	182	32	0.88	0.77	0.11
225	19	344	261	82	175	140	34	0.48	0.35	0.13
244	19	306	181	125	178	103	75	0.40	0.24	0.17
266	19	259	188	71	134	99	34	0.29	0.21	0.08
285	19	163	124	39	79	61	18	0.22	0.18	0.04

Day of Year	Station	[-- Fresh Weight ---]		[--- Dry Weight ----]		[----- LAI -----]				
		Total Grass	Non-Grass	Total Grass	Non-Grass	Total Grass	Non-Grass			
		[----- g/m2 -----]				[----- m2/m2 -----]				
119	20	0	0	0	0	0	0	0.00	0.00	0.00
132	20	130	80	50	40	26	14	0.22	0.16	0.06
138	20	272	234	38	85	75	11	0.56	0.51	0.06
152	20	521	397	124	163	128	35	1.04	0.86	0.18
166	20	404	351	53	176	148	29	0.80	0.72	0.07
180	20	507	386	121	280	225	55	0.71	0.55	0.16
194	20	476	404	72	216	183	33	1.05	0.93	0.12
208	20	521	462	59	253	225	29	1.08	0.98	0.09
222	20	365	344	21	188	179	10	0.44	0.41	0.02
236	20	477	444	33	189	175	14	0.76	0.74	0.02
258	20	230	209	21	146	135	12	0.15	0.14	0.01
280	20	303	292	10	178	168	10	0.29	0.28	0.01

Day of Year	Station	[-- Fresh Weight ---]		[--- Dry Weight ----]		[----- LAI -----]				
		Total Grass	Non-Grass	Total Grass	Non-Grass	Total Grass	Non-Grass			
		[----- g/m2 -----]				[----- m2/m2 -----]				
112	21	44	29	15	19	14	5	0.09	0.07	0.03
130	21	208	118	91	75	46	29	0.26	0.15	0.11
145	21	317	203	115	106	74	33	0.46	0.28	0.18
159	21	229	125	104	105	68	38	0.35	0.18	0.17
174	21	171	85	86	108	60	48	0.27	0.13	0.15
189	21	287	75	213	130	41	90	0.41	0.14	0.27
202	21	182	133	49	88	68	20	0.35	0.27	0.08
216	21	148	69	79	89	48	42	0.23	0.12	0.11
230	21	279	102	177	121	52	69	0.41	0.14	0.26
246	21	142	59	84	92	43	49	0.15	0.05	0.10
273	21	161	35	126	68	16	53	0.20	0.06	0.15
294	21	28	3	25	17	2	15	0.02	0.00	0.02

Day of Year	Station	[-- Fresh Weight ---]		[--- Dry Weight ----]		[----- LAI -----]				
		Total Grass	Non-Grass	Total Grass	Non-Grass	Total Grass	Non-Grass			
		[----- g/m2 -----]				[----- m2/m2 -----]				
110	23	0	0	0	0	0	0	0.00	0.00	0.00
124	23	97	83	14	26	23	3	0.17	0.15	0.02
139	23	305	210	95	96	69	26	0.62	0.43	0.19
159	23	365	257	108	134	97	38	0.83	0.59	0.24
173	23	281	207	74	126	97	29	0.55	0.42	0.14
187	23	282	191	91	129	86	43	0.57	0.44	0.13
200	23	347	245	102	138	99	39	0.92	0.67	0.24
214	23	276	193	82	161	111	50	0.53	0.38	0.14
228	23	331	233	98	164	116	49	0.69	0.45	0.24
244	23	160	108	52	103	71	32	0.24	0.14	0.10
267	23	238	83	155	116	45	71	0.33	0.14	0.18
293	23	27	20	8	20	16	4	0.03	0.02	0.01

Day of Year	Station	[-- Fresh Weight ---]		[--- Dry Weight ----]		[----- LAI -----]				
		Total Grass	Non-Grass	Total Grass	Non-Grass	Total Grass	Non-Grass			
		[----- g/m2 -----]						[----- m2/m2 -----]		
112	25	101	90	11	43	39	4	0.23	0.21	0.03
134	25	222	182	40	97	83	13	0.36	0.28	0.08
144	25	436	369	67	152	137	14	0.62	0.51	0.11
158	25	315	215	100	129	93	36	0.60	0.47	0.13
173	25	252	179	73	138	102	36	0.42	0.34	0.09
187	25	311	132	179	130	65	65	0.54	0.28	0.26
200	25	305	183	122	114	69	45	0.77	0.54	0.23
214	25	207	113	94	116	70	46	0.37	0.24	0.13
228	25	252	87	165	114	48	66	0.33	0.14	0.20
244	25	189	14	175	90	9	81	0.23	0.03	0.20
270	25	236	23	213	104	10	94	0.26	0.04	0.22
294	25	52	9	43	24	4	20	0.04	0.02	0.02

Day of Year	Station	[-- Fresh Weight ---]		[--- Dry Weight ----]		[----- LAI -----]				
		Total Grass	Non-Grass	Total Grass	Non-Grass	Total Grass	Non-Grass			
		[----- g/m2 -----]						[----- m2/m2 -----]		
114	27	0	0	0	0	0	0	0.00	0.00	0.00
124	27	140	135	5	37	36	1	0.24	0.24	0.01
141	27	308	139	170	111	63	48	0.47	0.27	0.20
158	27	374	242	132	136	95	41	0.81	0.63	0.18
173	27	307	186	121	137	91	46	0.54	0.35	0.19
188	27	321	216	105	147	102	45	0.55	0.42	0.14
201	27	323	256	66	128	106	22	0.79	0.67	0.11
215	27	497	220	277	245	119	126	0.72	0.41	0.31
229	27	561	215	346	246	109	138	0.81	0.33	0.48
246	27	228	120	108	135	75	61	0.26	0.16	0.09
271	27	153	118	35	85	66	19	0.21	0.18	0.03
291	27	72	57	14	44	36	8	0.07	0.06	0.02

Day of Year	Station	[-- Fresh Weight ---]		[--- Dry Weight ----]		[----- LAI -----]				
		Total Grass	Non-Grass	Total Grass	Non-Grass	Total Grass	Non-Grass			
		[----- g/m2 -----]						[----- m2/m2 -----]		
116	29	87	56	31	27	21	7	0.12	0.09	0.03
126	29	40	24	17	19	13	6	0.08	0.05	0.03
139	29	185	144	41	65	54	12	0.32	0.25	0.07
154	29	374	242	132	132	85	47	0.82	0.53	0.28
168	29	239	171	68	103	74	29	0.52	0.34	0.18
182	29	287	265	22	125	116	9	0.62	0.58	0.04
196	29	311	243	68	169	130	39	0.77	0.58	0.19
210	29	323	278	46	158	131	27	0.71	0.57	0.14
224	29	238	212	26	129	118	12	0.31	0.25	0.05
239	29	275	200	75	147	111	36	0.43	0.32	0.11
263	29	126	112	14	67	61	6	0.17	0.15	0.02
286	29	119	86	34	64	49	15	0.16	0.12	0.04

Day of Year	Station	[-- Fresh Weight ---]			[--- Dry Weight ----]			[----- LAI -----]		
		Total	Grass	Non-Grass	Total	Grass	Non-Grass	Total	Grass	Non-Grass
		[----- g/m2 -----]						[----- m2/m2 -----]		
112	31	48	21	27	28	14	14	0.10	0.07	0.04
132	31	295	43	252	159	25	134	0.37	0.07	0.30
141	31	157	102	54	71	51	20	0.28	0.18	0.10
159	31	636	417	218	223	162	60	1.20	0.87	0.33
174	31	485	346	139	206	167	39	0.83	0.60	0.23
189	31	649	412	237	275	186	90	1.44	0.95	0.49
202	31	970	611	359	393	262	131	1.96	1.43	0.54
216	31	592	490	102	268	221	47	1.36	1.05	0.30
230	31	430	417	14	202	196	7	0.95	0.92	0.02
246	31	343	304	40	180	162	19	0.60	0.54	0.06
273	31	332	265	67	141	111	30	0.49	0.40	0.09
295	31	125	35	91	74	17	57	0.08	0.06	0.03

Day of Year	Station	[-- Fresh Weight ---]			[--- Dry Weight ----]			[----- LAI -----]		
		Total	Grass	Non-Grass	Total	Grass	Non-Grass	Total	Grass	Non-Grass
		[----- g/m2 -----]						[----- m2/m2 -----]		
116	36	99	55	44	35	23	12	0.18	0.11	0.06
134	36	197	122	75	78	53	24	0.31	0.18	0.13
144	36	299	193	105	119	82	37	0.59	0.36	0.23
158	36	397	145	252	157	63	94	0.93	0.30	0.63
174	36	206	157	49	111	89	22	0.29	0.22	0.07
188	36	279	151	129	137	81	56	0.49	0.31	0.17
201	36	279	198	81	111	81	31	0.63	0.47	0.15
215	36	171	120	51	103	79	24	0.35	0.27	0.08
229	36	118	66	52	64	39	25	0.16	0.09	0.07
245	36	131	66	66	72	41	31	0.16	0.07	0.09
271	36	87	37	50	50	23	27	0.10	0.05	0.05
292	36	34	8	26	18	4	14	0.02	0.01	0.02

Day of Year	Station	[-- Fresh Weight ---]			[--- Dry Weight ----]			[----- LAI -----]		
		Total	Grass	Non-Grass	Total	Grass	Non-Grass	Total	Grass	Non-Grass
		[----- g/m2 -----]						[----- m2/m2 -----]		
110	40	0	0	0	0	0	0	0.00	0.00	0.00
126	40	83	39	44	22	13	9	0.11	0.07	0.04
139	40	214	132	83	77	54	22	0.34	0.22	0.12
154	40	413	284	128	145	104	41	1.01	0.68	0.33
168	40	305	278	27	126	117	10	0.63	0.57	0.06
182	40	255	201	54	116	95	21	0.54	0.46	0.08
196	40	378	313	64	175	145	31	0.93	0.79	0.14
210	40	313	280	33	148	132	16	0.70	0.62	0.07
224	40	340	240	100	176	130	46	0.45	0.36	0.09
239	40	328	197	131	178	115	63	0.47	0.36	0.12
263	40	373	174	200	180	91	89	0.48	0.28	0.19
286	40	148	82	67	96	53	43	0.20	0.13	0.06

Day of [% Water by Weight]
 Year Station 0-5 5-10 0-10
 [---- g/g x 100 ----]

102	2	0.0	0.0	0.0
117	2	19.8	24.6	22.2
125	2	26.2	21.3	23.8
138	2	10.4	17.0	13.7
146	2	37.5	29.4	33.5
154	2	27.6	24.7	26.2
159	2	14.6	17.7	16.2
169	2	16.6	15.7	16.1
175	2	11.0	16.1	13.5
182	2	29.5	20.6	25.0
190	2	14.6	17.8	16.2
196	2	20.1	22.7	21.4
203	2	20.0	20.9	20.4
209	2	13.0	17.9	15.4
216	2	11.8	15.1	13.5
223	2	13.9	14.6	14.2
230	2	15.9	19.3	17.6
245	2	12.2	16.1	14.2
260	2	16.0	11.1	13.6
272	2	24.0	16.9	20.4
294	2	17.1	15.2	16.1

Day of [% Water by Weight]
 Year Station 0-5 5-10 0-10
 [---- g/g x 100 ----]

106	5	38.3	34.2	36.2
117	5	32.3	31.6	32.0
125	5	38.5	31.3	34.9
138	5	17.3	23.0	20.1
146	5	39.6	33.9	36.8
154	5	34.1	26.8	30.5
159	5	20.1	22.1	21.1
169	5	24.0	18.5	21.3
175	5	14.7	17.1	15.9
182	5	40.5	32.7	36.6
190	5	19.1	21.8	20.5
196	5	26.7	26.1	26.4
203	5	26.3	23.9	25.1
209	5	16.9	19.9	18.4
216	5	14.7	16.1	15.4
223	5	15.2	15.2	15.2
230	5	25.9	25.9	25.9
245	5	16.5	17.9	17.2
260	5	14.9	13.5	14.2
272	5	36.4	27.9	32.1
294	5	28.6	21.4	25.0

Day of [% Water by Weight]
 Year Station 0-5 5-10 0-10
 [---- g/g x 100 ----]

102	6	0.0	0.0	0.0
111	6	0.0	0.0	0.0
125	6	39.7	29.6	34.7
138	6	27.2	24.0	25.6
146	6	36.4	6.3	21.3
154	6	36.9	0.0	18.5
159	6	30.5	25.6	28.1
167	6	35.3	21.1	28.2
175	6	21.9	13.6	17.8
183	6	42.3	27.9	35.1
193	6	40.3	29.8	35.1
200	6	39.9	28.2	34.0
204	6	31.4	25.9	28.7
210	6	24.3	15.3	19.8
217	6	18.6	4.7	11.6
224	6	12.3	3.1	7.7
231	6	21.0	13.5	17.2
246	6	16.7	4.7	10.7
260	6	23.4	3.0	13.2
274	6	16.8	4.5	10.7
295	6	23.1	4.4	13.7

Day of [% Water by Weight]
 Year Station 0-5 5-10 0-10
 [---- g/g x 100 ----]

106	7	34.9	13.2	24.1
117	7	34.4	35.4	34.9
125	7	35.1	28.0	31.6
138	7	21.4	22.1	21.8
146	7	34.5	13.4	24.0
155	7	30.6	18.9	24.8
159	7	22.8	27.3	25.0
167	7	25.8	4.3	15.1
175	7	16.6	13.3	15.0
183	7	35.2	11.0	23.1
190	7	20.5	8.6	14.5
197	7	21.5	17.3	19.4
204	7	24.0	17.1	20.6
210	7	14.7	12.7	13.7
216	7	14.7	12.0	13.3
224	7	13.6	17.0	15.3
231	7	19.1	9.3	14.2
246	7	16.6	11.4	14.0
260	7	18.1	15.4	16.7
274	7	21.6	10.6	16.1
295	7	23.8	18.6	21.2

Day of [% Water by Weight]
 Year Station 0-5 5-10 0-10
 [---- g/g x 100 ----]

102	8	0.0	0.0	0.0
117	8	25.2	17.2	21.2
125	8	28.1	16.8	22.4
138	8	13.5	12.6	13.0
146	8	40.8	26.1	33.4
155	8	30.5	15.2	22.9
159	8	20.4	9.0	14.7
167	8	23.9	3.2	13.5
175	8	9.7	6.0	7.8
183	8	41.0	15.5	28.3
193	8	44.9	13.7	29.3
197	8	21.1	10.5	15.8
204	8	23.6	10.3	17.0
210	8	17.7	7.1	12.4
216	8	9.1	2.4	5.8
224	8	9.4	2.1	5.7
231	8	18.4	8.4	13.4
246	8	11.4	2.8	7.1
260	8	16.9	2.1	9.5
274	8	19.3	2.1	10.7
295	8	18.7	2.7	10.7

Day of [% Water by Weight]
 Year Station 0-5 5-10 0-10
 [---- g/g x 100 ----]

102	10	0.0	0.0	0.0
111	10	0.0	0.0	0.0
123	10	0.0	0.0	0.0
139	10	27.6	7.2	17.4
146	10	42.8	22.1	32.5
155	10	35.6	5.7	20.6
158	10	0.0	0.0	0.0
166	10	20.6	11.3	15.9
176	10	19.2	9.9	14.6
183	10	38.8	15.0	26.9
190	10	25.0	5.7	15.4
197	10	23.8	15.5	19.7
203	10	31.0	14.0	22.5
210	10	23.3	3.9	13.6
216	10	18.5	8.5	13.5
224	10	17.6	8.2	12.9
231	10	23.5	5.7	14.6
246	10	18.7	9.4	14.0
260	10	20.6	7.7	14.1
274	10	14.9	7.4	11.2
295	10	29.3	16.7	23.0

Day of [% Water by Weight]
 Year Station 0-5 5-10 0-10
 [---- g/g x 100 ----]

102	11	0.0	0.0	0.0
119	11	29.1	30.8	30.0
126	11	31.6	29.8	30.7
140	11	13.6	21.0	17.3
147	11	40.9	32.9	36.9
153	11	30.5	26.8	28.6
160	11	16.9	22.2	19.6
168	11	18.8	17.8	18.3
174	11	12.6	16.9	14.8
181	11	10.8	15.2	13.0
188	11	22.2	22.6	22.4
195	11	31.0	26.8	28.9
202	11	30.8	26.2	28.5
208	11	14.7	17.5	16.1
215	11	12.4	15.8	14.1
222	11	12.5	13.8	13.2
230	11	20.4	21.2	20.8
242	11	14.0	15.8	14.9
256	11	9.9	14.1	12.0
270	11	19.6	19.7	19.7
291	11	14.0	17.3	15.7

Day of [% Water by Weight]
 Year Station 0-5 5-10 0-10
 [---- g/g x 100 ----]

102	12	0.0	0.0	0.0
111	12	0.0	0.0	0.0
125	12	34.0	12.9	23.5
138	12	16.9	13.4	15.1
146	12	41.4	31.6	36.5
154	12	41.4	21.7	31.6
159	12	24.9	12.1	18.5
167	12	27.7	5.3	16.5
175	12	15.8	3.9	9.9
183	12	40.3	6.6	23.4
193	12	33.5	18.8	26.2
200	12	32.8	17.9	25.4
204	12	25.5	14.4	19.9
210	12	17.9	4.6	11.3
217	12	21.7	19.2	20.5
224	12	20.3	15.9	18.1
231	12	27.3	21.8	24.5
246	12	23.9	18.6	21.3
260	12	23.4	12.1	17.8
274	12	26.0	18.5	22.2
295	12	36.4	18.4	27.4

Day of [% Water by Weight]
 Year Station 0-5 5-10 0-10
 [----- g/g x 100 -----]

103	13	29.2	28.5	28.9
116	13	27.3	24.4	25.8
124	13	38.4	22.5	30.4
138	13	18.3	18.2	18.3
147	13	37.0	26.6	31.8
154	13	27.8	21.1	24.5
160	13	16.6	16.5	16.5
168	13	20.0	14.5	17.3
174	13	14.0	15.0	14.5
181	13	11.4	13.3	12.4
189	13	17.3	17.2	17.3
196	13	22.4	20.8	21.6
203	13	22.2	20.8	21.5
209	13	13.9	15.0	14.5
216	13	15.0	14.8	14.9
223	13	12.9	13.5	13.2
231	13	14.8	15.0	14.9
244	13	14.0	14.5	14.3
258	13	7.7	12.3	10.0
273	13	27.5	15.5	21.5
293	13	14.0	14.5	14.2

Day of [% Water by Weight]
 Year Station 0-5 5-10 0-10
 [----- g/g x 100 -----]

102	14	0.0	0.0	0.0
111	14	0.0	0.0	0.0
123	14	0.0	0.0	0.0
139	14	31.9	18.9	25.4
146	14	43.4	13.4	28.4
155	14	39.4	6.7	23.1
158	14	0.0	0.0	0.0
166	14	24.0	16.0	20.0
176	14	19.8	13.4	16.6
183	14	38.1	20.1	29.1
190	14	29.4	5.4	17.4
197	14	25.9	6.3	16.1
203	14	27.2	11.7	19.5
210	14	21.4	0.0	10.7
216	14	17.5	9.9	13.7
224	14	16.1	8.5	12.3
231	14	23.2	10.7	17.0
246	14	18.8	4.7	11.7
260	14	19.8	4.4	12.1
274	14	16.4	3.2	9.8
295	14	29.2	4.2	16.7

Day of [% Water by Weight]
 Year Station 0-5 5-10 0-10
 [----- g/g x 100 -----]

102	17	40.1	34.6	37.4
111	17	35.1	31.5	33.3
123	17	20.5	25.0	22.7
137	17	14.6	20.6	17.6
145	17	41.0	33.2	37.1
152	17	20.0	22.5	21.3
158	17	20.0	20.4	20.2
165	17	16.0	17.2	16.6
172	17	15.0	17.1	16.0
181	17	15.2	8.8	12.0
187	17	24.9	16.4	20.7
194	17	28.8	25.9	27.4
202	17	27.3	25.1	26.2
208	17	14.5	17.9	16.2
215	17	11.5	15.4	13.5
222	17	18.9	13.9	16.4
229	17	24.3	21.9	23.1
238	17	20.5	18.9	19.7
251	17	12.0	15.2	13.6
265	17	25.0	18.7	21.9
284	17	21.1	19.6	20.4

Day of [% Water by Weight]
 Year Station 0-5 5-10 0-10
 [----- g/g x 100 -----]

102	19	50.9	35.0	42.9
111	19	45.4	36.8	41.1
124	19	38.5	23.2	30.9
137	19	14.1	15.6	14.8
145	19	46.6	33.4	40.0
152	19	22.3	22.1	22.2
158	19	17.7	17.3	17.5
165	19	11.7	12.9	12.3
172	19	11.7	12.2	11.9
181	19	9.6	11.7	10.6
187	19	19.8	14.6	17.2
194	19	32.3	25.7	29.0
202	19	24.9	21.9	23.4
208	19	12.2	13.1	12.7
215	19	13.2	11.2	12.2
222	19	20.3	13.9	17.1
229	19	16.1	14.1	15.1
238	19	19.1	14.1	16.6
251	19	9.3	11.2	10.3
265	19	23.3	16.3	19.8
284	19	19.5	14.7	17.1

Day of [% Water by Weight]
 Year Station 0-5 5-10 0-10
 [---- g/g x 100 ----]

102	20	0.0	0.0	0.0
119	20	23.8	19.7	21.8
127	20	31.5	26.4	29.0
140	20	16.4	16.5	16.5
148	20	30.8	28.2	29.5
153	20	24.2	22.4	23.3
160	20	16.8	18.9	17.9
168	20	20.8	16.6	18.7
174	20	13.7	15.8	14.7
181	20	11.6	14.3	13.0
188	20	17.7	17.5	17.6
195	20	25.9	23.6	24.8
202	20	28.4	25.4	26.9
208	20	16.3	17.7	17.0
215	20	14.9	15.8	15.3
222	20	14.8	14.5	14.7
229	20	21.0	18.6	19.8
239	20	18.3	17.3	17.8
253	20	10.9	14.3	12.6
267	20	18.9	18.1	18.5
286	20	15.5	16.6	16.1

Day of [% Water by Weight]
 Year Station 0-5 5-10 0-10
 [---- g/g x 100 ----]

102	21	43.6	36.0	39.8
111	21	38.3	32.0	35.2
126	21	28.6	24.8	26.7
137	21	11.1	17.8	14.5
145	21	45.6	34.7	40.1
152	21	19.2	24.5	21.9
158	21	13.4	18.1	15.8
165	21	9.7	14.4	12.0
173	21	9.2	14.3	11.8
181	21	6.9	13.1	10.0
187	21	23.4	21.5	22.4
194	21	30.2	27.4	28.8
202	21	29.2	26.6	27.9
208	21	13.3	16.5	14.9
215	21	10.6	13.4	12.0
222	21	20.1	17.1	18.6
229	21	13.3	15.6	14.5
239	21	11.0	11.2	11.1
253	21	7.8	12.3	10.0
265	21	19.8	13.8	16.8
284	21	12.5	13.9	13.2

Day of [% Water by Weight]
 Year Station 0-5 5-10 0-10
 [---- g/g x 100 ----]

103	23	36.6	33.8	35.2
111	23	36.3	32.5	34.4
124	23	35.8	25.8	30.8
137	23	14.0	18.1	16.1
145	23	44.4	34.0	39.2
152	23	21.8	24.8	23.3
158	23	16.3	19.8	18.1
165	23	12.6	15.6	14.1
173	23	13.6	14.6	14.1
181	23	9.2	12.5	10.8
188	23	21.6	20.6	21.1
194	23	24.3	22.2	23.3
202	23	29.2	25.4	27.3
208	23	14.0	16.3	15.2
215	23	9.5	12.5	11.0
222	23	16.4	13.0	14.7
230	23	14.0	14.2	14.1
239	23	10.4	12.8	11.6
253	23	8.8	11.6	10.2
267	23	19.8	18.5	19.2
286	23	12.2	13.8	13.0

Day of [% Water by Weight]
 Year Station 0-5 5-10 0-10
 [---- g/g x 100 ----]

103	25	37.9	32.6	35.2
116	25	24.5	24.2	24.4
124	25	35.0	19.2	27.1
137	25	14.0	12.8	13.4
145	25	54.4	20.8	37.6
152	25	18.7	14.5	16.6
158	25	16.3	12.2	14.3
165	25	14.5	9.5	12.0
173	25	12.4	11.0	11.7
181	25	10.3	9.4	9.8
188	25	26.1	12.6	19.4
195	25	29.7	14.6	22.2
203	25	29.6	21.8	25.7
208	25	15.3	14.1	14.7
215	25	12.2	8.4	10.3
222	25	13.3	10.2	11.8
230	25	18.5	12.7	15.6
239	25	16.4	8.7	12.6
253	25	10.7	10.8	10.8
267	25	21.4	14.8	18.1
286	25	14.1	12.1	13.1

Day of [% Water by Weight]
 Year Station 0-5 5-10 0-10
 [----- g/g x 100 -----]

103	27	29.6	27.7	28.7
117	27	22.0	28.8	25.4
127	27	16.7	0.0	8.4
137	27	16.0	10.6	13.3
145	27	33.1	12.1	22.6
152	27	0.0	0.0	0.0
159	27	16.9	11.2	14.0
165	27	13.6	9.2	11.4
173	27	8.2	3.0	5.6
181	27	10.3	7.4	8.9
188	27	20.6	12.6	16.6
195	27	23.7	13.8	18.8
203	27	22.8	14.5	18.6
209	27	15.2	11.3	13.2
217	27	11.3	5.4	8.4
224	27	11.0	9.5	10.2
230	27	19.6	16.2	17.9
242	27	12.5	6.2	9.4
256	27	11.2	5.4	8.3
270	27	17.3	12.1	14.7
291	27	13.4	12.1	12.8

Day of [% Water by Weight]
 Year Station 0-5 5-10 0-10
 [----- g/g x 100 -----]

106	29	31.5	30.3	30.9
119	29	22.3	23.7	23.0
126	29	29.1	25.4	27.2
139	29	12.0	17.3	14.7
147	29	39.8	32.2	36.0
153	29	21.8	24.4	23.1
160	29	15.9	20.5	18.2
168	29	24.9	17.1	21.0
174	29	13.0	17.1	15.1
181	29	10.1	15.5	12.8
189	29	17.2	19.3	18.2
195	29	28.9	26.0	27.4
203	29	28.0	22.9	25.4
209	29	15.3	19.1	17.2
216	29	1.9	2.9	2.4
223	29	12.7	13.9	13.3
231	29	18.8	21.7	20.2
244	29	13.5	13.1	13.3
258	29	10.1	13.9	12.0
273	29	34.6	26.9	30.8
293	29	13.5	16.6	15.1

Day of [% Water by Weight]
 Year Station 0-5 5-10 0-10
 [----- g/g x 100 -----]

103	31	43.7	7.1	25.4
117	31	39.4	31.8	35.6
127	31	37.1	15.8	26.5
140	31	15.3	12.4	13.9
148	31	37.0	7.1	22.1
154	31	34.2	7.0	20.6
159	31	26.6	11.7	19.2
167	31	34.0	20.5	27.2
174	31	20.1	8.1	14.1
181	31	15.1	6.5	10.8
188	31	27.8	16.3	22.0
195	31	31.8	11.5	21.6
204	31	28.3	5.2	16.8
210	31	20.7	9.0	14.9
217	31	19.1	9.6	14.4
224	31	16.0	13.1	14.5
231	31	24.7	4.4	14.5
246	31	18.5	3.5	11.0
260	31	32.2	7.9	20.1
274	31	31.9	6.1	19.0
295	31	35.2	14.9	25.1

Day of [% Water by Weight]
 Year Station 0-5 5-10 0-10
 [----- g/g x 100 -----]

102	36	0.0	0.0	0.0
119	36	20.1	26.2	23.1
124	36	29.4	22.2	25.8
137	36	13.8	18.0	15.9
145	36	45.4	34.2	39.8
154	36	37.9	27.1	32.5
159	36	19.4	22.3	20.9
165	36	14.5	18.2	16.3
173	36	12.2	16.6	14.4
181	36	10.4	15.3	12.9
188	36	23.2	22.5	22.9
195	36	25.9	25.7	25.8
202	36	24.9	24.5	24.7
208	36	12.2	17.4	14.8
215	36	11.3	14.9	13.1
222	36	15.4	13.6	14.5
230	36	19.4	20.0	19.7
242	36	13.1	15.9	14.5
256	36	9.6	13.8	11.7
270	36	16.6	17.7	17.2
291	36	13.0	15.6	14.3

Day of [% Water by Weight]
 Year Station 0-5 5-10 0-10
 [---- g/g x 100 ----]

102	40	0.0	0.0	0.0
119	40	24.7	20.8	22.8
126	40	26.6	23.2	24.9
139	40	16.5	8.6	12.5
147	40	30.2	19.0	24.6
154	40	35.0	6.1	20.6
160	40	18.0	9.5	13.7
168	40	26.2	16.9	21.6
174	40	16.4	12.2	14.3
181	40	13.2	14.1	13.7
189	40	18.4	12.7	15.6
195	40	29.3	23.8	26.5
203	40	25.4	21.2	23.3
209	40	20.7	13.5	17.1
216	40	14.7	10.9	12.8
223	40	13.2	10.6	11.9
231	40	17.6	20.7	19.2
244	40	15.9	15.4	15.6
258	40	12.9	13.9	13.4
273	40	30.6	10.6	20.6
293	40	16.1	15.1	15.6

Day of		[----- mm of Water -----]					
Year	Stat.	Mean	Tube-1	Tube-2	Tube-3	Tube-4	Tube-5
102	2	0	0	0	0	0	0
117	2	272	287	250	349	344	130
125	2	267	285	240	345	343	122
139	2	249	267	228	325	331	97
146	2	247	278	227	293	332	105
154	2	243	265	223	319	329	79
159	2	242	256	216	316	326	95
169	2	235	249	204	308	320	91
175	2	236	244	235	301	313	87
182	2	231	245	201	299	311	97
190	2	225	240	196	294	303	92
196	2	247	252	236	305	316	125
203	2	243	250	227	305	313	118
209	2	236	246	219	303	311	101
216	2	225	239	205	293	298	92
223	2	220	237	194	287	293	89
230	2	229	239	219	290	295	102
245	2	229	237	239	283	291	92
260	2	0	0	0	0	0	0
272	2	243	232	251	354	270	106
294	2	263	255	259	347	338	114

Day of		[----- mm of Water -----]					
Year	Stat.	Mean	Tube-1	Tube-2	Tube-3	Tube-4	Tube-5
106	5	138	148	0	129	0	0
118	5	124	132	0	116	0	0
125	5	134	130	0	138	0	0
139	5	115	121	0	108	0	0
146	5	122	128	0	116	0	0
154	5	126	143	0	109	0	0
159	5	109	116	0	102	0	0
169	5	98	104	0	92	0	0
175	5	102	103	0	102	0	0
182	5	104	117	0	91	0	0
190	5	88	93	0	83	0	0
196	5	104	109	0	99	0	0
203	5	108	122	0	95	0	0
209	5	102	116	0	88	0	0
216	5	94	107	0	82	0	0
223	5	93	107	0	79	0	0
230	5	100	113	0	87	0	0
245	5	102	108	0	96	0	0
260	5	0	0	0	0	0	0
272	5	108	118	0	99	0	0
294	5	110	112	0	108	0	0

Day of		[----- mm of Water -----]					
Year	Stat.	Mean	Tube-1	Tube-2	Tube-3	Tube-4	Tube-5
102	11	0	0	0	0	0	0
119	11	0	0	0	0	0	0
126	11	253	308	245	269	177	264
140	11	252	310	243	274	171	263
147	11	265	318	249	289	189	282
153	11	264	321	245	287	189	278
160	11	258	318	240	280	183	270
168	11	249	307	230	275	173	262
174	11	237	306	223	268	134	256
181	11	233	295	209	260	154	245
189	11	242	294	210	304	155	246
195	11	237	293	212	271	160	249
202	11	236	296	209	268	161	244
208	11	232	292	206	263	156	242
217	11	223	285	196	255	146	236
222	11	222	284	192	253	144	235
230	11	223	285	193	256	146	233
242	11	219	281	189	251	143	229
256	11	215	280	183	246	140	226
270	11	218	281	189	252	143	226
291	11	290	379	242	329	190	307

Day of		[----- mm of Water -----]					
Year	Stat.	Mean	Tube-1	Tube-2	Tube-3	Tube-4	Tube-5
105	13	357	398	0	0	315	0
116	13	305	345	0	264	0	0
124	13	304	308	0	0	300	0
138	13	0	0	0	0	0	0
147	13	328	345	345	343	268	338
154	13	323	340	346	338	261	331
160	13	319	334	344	334	256	329
168	13	309	318	333	325	249	321
174	13	306	310	334	323	244	316
181	13	297	299	323	316	237	308
189	13	280	292	318	205	0	305
196	13	298	300	321	314	250	307
203	13	289	292	316	315	218	304
209	13	282	285	310	305	212	299
216	13	277	283	301	301	205	294
223	13	271	275	294	291	199	294
231	13	268	275	289	288	200	290
244	13	261	271	283	278	193	281
258	13	256	271	272	265	190	282
273	13	311	294	330	326	0	294
293	13	343	382	378	375	247	335

Day of		[----- mm of Water -----]					
Year	Stat.	Mean	Tube-1	Tube-2	Tube-3	Tube-4	Tube-5
105	17	267	253	224	363	229	0
111	17	252	241	220	326	223	0
124	17	231	216	190	328	192	0
137	17	216	213	159	304	188	0
145	17	222	207	177	319	184	0
151	17	223	203	179	326	182	0
157	17	224	0	172	321	180	0
165	17	200	180	167	284	169	0
172	17	199	170	165	303	161	0
181	17	188	163	156	282	149	0
187	17	190	167	159	282	153	0
194	17	208	189	164	309	168	0
202	17	204	190	164	298	163	0
208	17	198	184	157	294	157	0
217	17	189	170	154	281	149	0
222	17	177	166	148	247	147	0
229	17	188	172	153	279	149	0
238	17	186	169	152	279	147	0
251	17	180	161	148	265	145	0
265	17	192	178	153	287	151	0
284	17	202	169	184	295	159	0

Day of		[----- mm of Water -----]					
Year	Stat.	Mean	Tube-1	Tube-2	Tube-3	Tube-4	Tube-5
103	19	225	225	0	0	0	0
111	19	203	203	0	0	0	0
124	19	198	198	0	0	0	0
137	19	194	194	0	0	0	0
145	19	190	190	0	0	0	0
151	19	190	190	0	0	0	0
157	19	186	186	0	0	0	0
165	19	173	173	0	0	0	0
172	19	162	162	0	0	0	0
181	19	0	0	0	0	0	0
187	19	151	151	0	0	0	0
194	19	173	173	0	0	0	0
202	19	173	173	0	0	0	0
208	19	166	166	0	0	0	0
217	19	161	161	0	0	0	0
222	19	153	153	0	0	0	0
229	19	155	155	0	0	0	0
238	19	157	157	0	0	0	0
251	19	145	145	0	0	0	0
265	19	160	160	0	0	0	0
284	19	128	128	0	0	0	0

Day of		[----- mm of Water -----]					
Year	Stat.	Mean	Tube-1	Tube-2	Tube-3	Tube-4	Tube-5
102	20	0	0	0	0	0	0
119	20	137	147	110	190	0	101
127	20	136	146	109	186	0	101
140	20	124	135	101	171	0	90
148	20	134	148	110	178	0	102
153	20	128	140	103	176	0	95
160	20	115	126	92	158	0	82
168	20	118	112	82	155	173	67
174	20	110	104	76	149	167	55
181	20	102	94	68	145	163	42
189	20	111	130	68	146	167	47
195	20	119	98	93	154	172	78
202	20	121	98	99	153	173	82
208	20	112	96	87	146	167	64
217	20	101	90	73	141	161	42
222	20	97	88	67	137	155	38
229	20	103	88	67	143	160	58
239	20	99	88	67	140	160	41
253	20	95	84	62	137	155	36
267	20	99	89	66	140	138	61
286	20	127	93	105	169	217	49

Day of		[----- mm of Water -----]					
Year	Stat.	Mean	Tube-1	Tube-2	Tube-3	Tube-4	Tube-5
105	21	238	266	224	261	175	264
111	21	233	267	226	261	178	232
126	21	214	230	194	260	155	230
137	21	199	222	186	219	146	222
145	21	201	226	189	220	152	219
151	21	199	222	189	214	151	219
157	21	191	212	181	205	143	212
165	21	177	199	169	194	126	198
173	21	164	186	160	182	113	182
181	21	157	177	150	176	105	178
187	21	162	179	154	182	114	184
194	21	182	198	180	200	131	203
202	21	188	200	184	205	138	212
208	21	177	190	172	194	126	204
217	21	162	176	155	180	109	190
222	21	162	176	157	181	109	185
229	21	169	177	170	185	118	194
239	21	159	174	157	177	103	183
253	21	152	167	148	172	97	176
265	21	164	180	141	187	115	195
284	21	170	193	140	193	118	204

Day of	[----- mm of Water -----]						
Year Stat.	Mean	Tube-1	Tube-2	Tube-3	Tube-4	Tube-5	
105	23	153	147	0	165	174	126
111	23	155	145	0	146	180	149
124	23	145	127	0	144	178	132
137	23	132	117	0	143	147	123
145	23	130	129	0	126	154	111
152	23	130	124	0	143	149	105
157	23	131	117	0	141	168	98
165	23	112	99	0	0	153	83
173	23	99	86	0	96	141	74
181	23	94	81	0	105	125	67
189	23	99	85	0	91	127	92
194	23	96	85	0	108	114	77
202	23	120	111	0	113	156	101
208	23	110	96	0	110	145	89
217	23	93	78	0	100	126	69
222	23	91	76	0	99	122	66
230	23	94	79	0	101	130	68
239	23	88	77	0	97	116	63
253	23	85	73	0	93	112	62
267	23	109	101	0	103	144	87
286	23	119	99	0	125	162	91

Day of	[----- mm of Water -----]						
Year Stat.	Mean	Tube-1	Tube-2	Tube-3	Tube-4	Tube-5	
106	29	135	0	173	107	0	125
119	29	120	0	147	110	102	121
126	29	124	0	170	109	99	119
139	29	98	0	138	78	84	94
147	29	118	0	147	112	103	110
153	29	117	0	143	107	99	121
160	29	107	0	137	103	90	99
168	29	104	0	132	94	82	109
174	29	88	0	124	67	76	84
181	29	84	0	114	79	71	74
189	29	95	0	118	85	85	94
195	29	110	0	130	107	98	104
203	29	101	0	127	84	95	100
209	29	87	0	102	74	82	90
216	29	81	0	110	64	73	79
223	29	77	0	107	61	69	71
231	29	83	0	115	68	69	82
244	29	74	0	109	64	60	63
258	29	69	0	103	59	57	56
273	29	81	0	128	62	64	70
293	29	77	0	111	66	67	65

Day of		[----- mm of Water -----]					
Year	Stat.	Mean	Tube-1	Tube-2	Tube-3	Tube-4	Tube-5
102	36	0	0	0	0	0	0
119	36	240	229	261	146	289	275
124	36	229	223	256	143	248	272
137	36	185	223	253	133	80	238
145	36	229	225	256	146	243	274
154	36	229	225	258	145	242	276
159	36	225	222	255	139	240	272
165	36	216	212	245	130	231	263
173	36	208	203	236	123	224	253
181	36	193	186	213	112	214	239
189	36	205	201	221	121	229	254
195	36	210	203	223	125	235	263
202	36	201	200	186	124	235	259
208	36	198	187	213	117	224	250
216	36	185	172	198	108	211	237
222	36	180	164	196	105	205	231
230	36	181	179	172	112	222	219
242	36	171	168	163	108	212	206
256	36	160	156	155	104	201	185
270	36	164	164	162	114	174	207
291	36	182	185	202	127	172	222